

12-2010

## Computational analysis for improved design of an SAE BAJA frame structure

Nagurbabu Noorbhasha  
*University of Nevada, Las Vegas*

Follow this and additional works at: <https://digitalscholarship.unlv.edu/thesesdissertations>



Part of the [Mechanical Engineering Commons](#)

---

### Repository Citation

Noorbhasha, Nagurbabu, "Computational analysis for improved design of an SAE BAJA frame structure" (2010). *UNLV Theses, Dissertations, Professional Papers, and Capstones*. 736.  
<https://digitalscholarship.unlv.edu/thesesdissertations/736>

This Thesis is protected by copyright and/or related rights. It has been brought to you by Digital Scholarship@UNLV with permission from the rights-holder(s). You are free to use this Thesis in any way that is permitted by the copyright and related rights legislation that applies to your use. For other uses you need to obtain permission from the rights-holder(s) directly, unless additional rights are indicated by a Creative Commons license in the record and/or on the work itself.

This Thesis has been accepted for inclusion in UNLV Theses, Dissertations, Professional Papers, and Capstones by an authorized administrator of Digital Scholarship@UNLV. For more information, please contact [digitalscholarship@unlv.edu](mailto:digitalscholarship@unlv.edu).

COMPUTATIONAL ANALYSIS FOR IMPROVED DESIGN OF AN SAE BAJA  
FRAME STRUCTURE

by

Nagurbabu Noorbhasha

Bachelor of Technology in Mechanical Engineering  
Jawaharlal Nehru Technological University, India  
April - 2003

A thesis submitted in partial fulfillment  
of the requirements for the

**Master of Science Degree in Mechanical Engineering**  
**Department of Mechanical Engineering**  
**Howard R. Hughes College of Engineering**

**Graduate College**  
**University of Nevada, Las Vegas**  
**December 2010**

Copyright by Nagurbabu Noorbhasha 2011  
All Rights Reserved



## THE GRADUATE COLLEGE

We recommend the thesis prepared under our supervision by

**Nagurbabu Noorbhasha**

entitled

**Computational Analysis for Improved Design of an SAE BAJA Frame Structure**

be accepted in partial fulfillment of the requirements for the degree of

**Master of Science in Mechanical Engineering**

Brendan J O'Toole, Committee Chair

Mohammed Trabia, Committee Member

Reynolds Douglas, Committee Member

Aly M Said,, Graduate Faculty Representative

Ronald Smith, Ph. D., Vice President for Research and Graduate Studies  
and Dean of the Graduate College

December 2010

## ABSTRACT

### **Computational Analysis for Improved Design of an SAE BAJA Frame Structure**

by

Nagurbabu Noorbhasha

Dr. Brendan J. O'Toole, Examination Committee Chair  
Associate Professor of Mechanical Engineering  
University of Nevada, Las Vegas

Baja SAE is an intercollegiate competition to design, fabricate, and race a small, single passenger, off-road vehicle powered by a 10 HP Briggs & Stratton 4-Stroke gasoline engine. All Baja SAE vehicles for the competition are powered by a small engine, thus large part of vehicle performance depends on the acceleration and maneuverability of the vehicle which is proportional to the weight of the chassis and rollcage. As weight is critical to achieve the greater performance of the vehicle, a balance must be found between the strength and weight of the rollcage to ensure the safety of the driver.

The objective of the present research was to optimize the design of roll cage in compliance with the guidelines set by SAE and to perform the finite element analysis (FEA) for validating the design. Initially, a preliminary design of the rollcage was produced based on the rules of the competition and a 3-D model was generated using CAD. To study the effects of stress and deformation on the frame members, linear static

frontal impact analysis was carried out using FEA techniques for different loading conditions on the rollcage model. The static analysis in this research is focused to obtain the optimum grid size for the rollcage structure. Modifications were done to the existing design to withstand the applied load based on the analysis results for the optimum mesh size. The design was considered to be safe if the generated roll-cage Von Mises stresses were less than the yield strength of the material and the deflections of the members were favorable enough for the safety of the driver. The research also presents different approaches to achieve the optimum design of the roll cage. The new design was subjected to FEA for validation.

Dynamic analysis was also performed on the vehicle chassis to review the structural rigidity of the chassis frame. A full vehicle modeling was carried out for the equivalent mass distribution of the vehicle. An initial velocity of 6.7 m/s (15 mph) is ascribed to the full vehicle model to impact a fixed rigid wall to investigate the effects of dynamic stresses, energy, reaction forces and acceleration of the frame members in a worst case loading scenario. Different ways of mitigating the acceleration on the chassis are also discussed in this research for the driver safety.

## ACKNOWLEDGEMENTS

I deeply express my sincere gratitude to my advisor Dr. Brendan J. O'Toole for trusting my abilities to work on this project. His invaluable guidance, suggestions, thoughts throughout the entire course of this research work is priceless. It has been very rewarding and satisfying experience to be able to work with him. I am also grateful to Department of Mechanical Engineering, University of Nevada Las Vegas for providing me the opportunity to pursue my master degree.

I would like to thank Dr. Mohamed B. Trabia, Dr. Reynolds Douglas and Dr. Aly M. Said for their time in reviewing the prospectus, participation in defense and counseling of the thesis as committee members.

Last but not the least, I would like to thank my parents, family and friends, and all the other people whom I have not mentioned above but have helped me in some way through the completion of my thesis degree. I would like to take this opportunity to express my gratitude to those who have helped me bring this thesis to a successful end with their knowledge, help and co-operation.

## TABLE OF CONTENTS

ABSTRACT .....	iii
ACKNOWLEDGEMENTS .....	v
LIST OF FIGURES .....	viii
LIST OF TABLES .....	ix
CHAPTER 1 INTRODUCTION .....	1
1.1 Background.....	1
1.2 SAE Baja Frame Design Objectives .....	2
1.3 Frontal Impact Testing.....	6
1.4 Objective of the Research.....	10
CHAPTER 2 FINITE ELEMENT ANALYSIS .....	12
2.1 Preprocessor Altair HyperMesh .....	12
2.2 Solver OptiStruct.....	14
2.3 Solver LS-DYNA.....	16
2.4 Post processor Altair HyperView .....	17
CHAPTER 3 LINEAR STATIC FRONTAL IMPACT ANALYSIS .....	20
3.1 Design Methodology.....	20
3.2 Development of a preliminary design .....	23
3.2.1 Design Guidelines .....	24
3.2.2 The Mini Baja Guidelines .....	25
3.2.3 Adequate Operator Space .....	25
3.3 Geometry Development.....	26
3.4 Material Selection .....	30
3.5 Linear Static Frontal Impact Analysis .....	33
3.5.1 Loading / Boundary Conditions.....	34
CHAPTER 4 RESULTS & DISCUSSION FOR THE STATIC ANALYSIS..	37
4.1 Grid Independence .....	37
4.2 Strengthening Mechanism .....	49
4.2.1 Providing gussets at the critical joints of the frame .....	50
4.2.2 Effect of gusset size on stress concentration .....	51
4.3 Load carrying capacity of the frame .....	56
4.4 Design modification .....	59
CHAPTER 5 DYNAMIC FRONTAL IMPACT ANALYSIS .....	62
5.1 Dynamic Analysis.....	62
5.2 Design Methodology for Dynamic Analysis .....	64



5.3 Geometry Development.....	65
5.4 Materials .....	66
5.4.1 *MAT_PLASTIC_KINEMATIC .....	67
5.5 Contact Surfaces .....	67
5.5.1 *CONTACT_TIED_SURFACE_TO_SURFACE.....	68
5.6 Rigid Wall.....	69
5.6.1 *RIGIDWALL_PLANAR .....	69
5.7 Loads and Boundary Conditions.....	69
5.7.1 INITIAL_VELOCITY_NODE.....	70
5.8 Frontal Impact Analysis Results Discussion:.....	71
CHAPTER 6 SUMMARY, CONCLUSION AND FUTURE WORK .....	78
6.1 Research Summary and Conclusion .....	78
6.2 Future Work.....	81
REFERENCES .....	82
APPENDIX A SAE BAJA RULES 2009 .....	85
APPENDIX B EXAMPLE LS-DYNA PROGRAM .....	96
VITA.....	99

## LIST OF FIGURES

Figure 1.1 Full width and frontal offset crash test.....	7
Figure 3.1 Flow chart for generic illustration of design process .....	22
Figure 3.2 Pro/Engineer model for the rollcage frame .....	27
Figure 3.3 HyperMesh model of the rollcage frame member.....	28
Figure 3.4 Magnified view of the meshed rollcage model.....	29
Figure 3.5 2D Element quality report.....	30
Figure 4.1 Mesh configuration for various grid sizes.....	40
Figure 4.2 Location of maximum Von Mises stress for various mesh sizes .....	42
Figure 4.3 Grid independence study graph for the max Von Mises stress .....	44
Figure 4.4 Grid independence study graph for the max displacement...	44
Figure 4.5 Selected locations of the points .....	45
Figure 4.6 Grid independence study graph for stress at selected locations .....	46
Figure 4.7 Grid independence study graph for displacement at selected locations.....	47
Figure 4.8 Provision of gussets at the frame joints .....	51
Figure 4.9 Effect of gusset size on the max Von Mises stress of the frame .....	55
Figure 4.10 Effect of gusset size on the max. displacement of the frame	55
Figure 4.11 Effect of impact load on maximum Von Mises stress .....	58
Figure 4.12 Effect of impact load on maximum displacement.....	58
Figure 4.13 New design of the chassis frame/rollcage .....	60
Figure 4.14 Von Mises stress distribution in the frame for 31138 N impact load .....	60
Figure 4.15 Displacement in the frame at 31138 N impact load .....	61
Figure 5.1 Chassis/Rollcage model for multi body dynamic analysis ....	66
Figure 5.2 Velocity profile of the rollcage structure.....	72
Figure 5.3 Rigid wall force history profile of the rollcage structure during the impact .....	73
Figure 5.4 Deformation of the frame members at different stages of impact.....	75
Figure 5.5 Energy plots for impact loading.....	75
Figure 5.6 Acceleration profiles during the impact .....	76

## LIST OF TABLES

Table 3.1 Material Property of the Frame .....	33
Table 4.1 Effect of maximum stress and displacement on mesh size ....	41
Table 4.2 Von Mises stress at selected locations after the impact loading .....	46
Table 4.3 Displacement of the frame at selected locations after the impact .....	47
Table 4.4 Effect of the mesh size on computation time & memory .....	48
Table 4.5 Effect of gusset size on the max. Von Mises stress of the frame .....	53
Table 4.6 Effect of gusset size on the max. displacement of the frame ..	54
Table 4.7 Effect of impact load on Von Mises stress and displacement .	57
Table 5.1 LS-DYNA material models.....	67

# CHAPTER 1

## INTRODUCTION

### 1.1 Background

SAE Baja is an intercollegiate engineering design competition for undergraduate and graduate engineering students organized by the Society of Automotive Engineers (SAE). The objective of the competition is to simulate real-world engineering design projects and their related challenges. A team of students (SAE BAJA team) has to design, fabricate, and race an off-road vehicle powered by a 10 HP Briggs and Stratton gasoline engine. Typical capabilities on basis of which these vehicles are judged are hill climb, load pull, rock crawl, acceleration, maneuverability and endurance on land as well as water.

All SAE approved Baja vehicles are required to use a 10 horsepower four-stroke engine. The engine cannot be enhanced in any way to ensure uniform comparison of overall vehicle design. Thus, a large part of vehicle performance depends on the drive train and the maneuverability of the vehicle. By improving drive-train efficiency, the vehicle will accelerate faster and achieve a higher top speed. The other contributing factor for the vehicle performance is acceleration and maneuverability. The total weight of the vehicle including the driver weight has significant impact on performance. Overall, a light vehicle should perform better since the engine capacity is fixed.

Driver safety is an important concern in the design of the vehicle. The rollage part of the chassis is the primary protection for the driver. So to ensure driver safety, the rollage must be structurally rigid. As weight is critical in a vehicle powered by a small engine, a balance must be found between the strength and weight of the vehicle. Thus the chassis design becomes very important in the vehicle performance.

## 1.2 SAE Baja Frame Design Objectives

The design of the SAE Baja frame is heavily influenced by the safety rules set out by the competition organizers. These rules are updated yearly to address new safety concerns. The frame design discussed in this report is in compliance with the 2009 Baja SAE Rules [1]. These rules define the frame design in two ways. First, the rules set specific requirements on minimum frame cross-section flexural strength. This flexural strength can be achieved by any combination of material and cross-section geometry. Smaller members can be used with stronger materials. They also define the specific requirements of the frame geometry, such as maximum length, width and height as well as minimum clearance between driver and frame members. The requirements were referenced when making decisions regarding the material selection, design geometry and any additional modifications to the design. A thorough review of the different types of chassis designs and rules were made at the end of the design stage before fabrication [2, 3, 4]. This review included not only the

letter of the guideline but also a discussion of the intent. In any cases in which the clarity or meaning of a rule was in doubt, the SAE rules committee was contacted to ensure compliance.

The following functional and design requirements were used as guides in the design process. Functionally, the vehicle should [5]:

1. Allow for easy driver entrance and exit
2. Be aesthetically pleasing
3. Be rugged, dependable, and easy to maintain
4. Be able to operate across rough terrain
5. Cost less than \$2,500
6. Maintain safety as a primary consideration

The scope of the design includes [5]:

1. A four-wheel vehicle with a roll cage with appropriate bracing which meets or exceeds all requirements of the SAE Mini Baja competition
2. Optimization of strength/weight ratio for the entire vehicle to enhance performance
3. A frame constructed of either steel tubing having a minimum carbon content of 0.18%, outside diameter of 0.0254 m (1.0 in.) and wall thickness of 0.0021 m (0.083 in.), or material having equivalent strength and bending modulus.

4. A frame designed to incorporate continuous lengths of tubing where possible to reduce welding and improve strength.
5. Consideration of the reliability and safety of all components, including frame, suspension, drive train, brakes, and steering

This vehicle was designed and to be produced with semi-skilled labor in a relatively high production volume, based on the concept of introducing a new product to the consumer industrial market from a fictitious company. The team uses learned engineering practices to design, build, test, and race this vehicle against other student teams, in a series of competitive events which reward teams for good engineering and mechanical practices. UNLV SAE Baja chassis/rollcage was designed to maximize strength and durability, while minimizing weight and retaining manufacturability [6]. The UNLV SAE BAJA team is relatively inexperienced compares to most of the schools in the competition. The team selected the cheapest steel tubing material readily available and selected the diameter and wall thickness to meet the minimum strength requirements specified in the rules. This resulted in a relatively weak material and large tubing dimensions than many competitors. The initial layout of the frame was chosen based on team members' best judgment and the dimensions of the tallest/biggest drivers. As team members learned the frame rules, additional members were added. The end result over a 3-year period is a frame that meets the design requirements

specified in the rules but was not optimal. It was not optimized because the team did not have the finances to purchase high strength steel and they did not have the analysis capability at the beginning of their design/fabrication phase. diameter and wall thickness to meet the mini

To best optimize the balance between strength, weight, durability and manufacturability, the use of Computer Aided Design (CAD) modeling and Finite Element Analysis (FEA) techniques are extremely useful in addition to conventional analysis. It covers the design constraints required by SAE, material selection, structural analysis and design modifications. It will finally cover the results of the actual real world usage of the frame design.

The frame configuration was designed to incorporate continuous tube lengths where possible. This helped to keep the frame as strong as possible, improved efficiency of material usage, reduced the number of welds required and reduced fabrication time.

The frame was constructed with the following important features [5]:

1. The firewall roll hoop was tilted back at an angle from the vertical for economy of space.
2. The roll cage widens front to back to increase passenger accessibility.
3. Tubing joint placements were optimized for greater strength of the roll cage.



4. Continuous sections of tubing were utilized where possible to increase the manufacturability of the frame by bending the tubing instead of welding the corners.
5. An adjustable seat to accommodate the height differences of drivers on the team

### 1.3 Frontal Impact Testing

The research indicates that most of the automotive fatalities or deaths occur due to head on or frontal crashes. In order to reduce traffic related fatalities and injuries, all the vehicles must pass frontal crash test. In the frontal impact or crash testing the vehicle crashes head-on into a rigid concrete barrier at certain specified speed. Federal law requires all passenger cars to pass a 13.4 m/s (30 mph) frontal crash test while the NCAP tests involve crashing a fixed barrier at 15.64 m/s (35 mph) [7]. Instrumented anthropomorphic dummies are placed in the driver and passenger seats for the test. Accelerometers are also placed on the vehicles to record response of structure during the crash. These tests are conducted to measure how well occupants are protected in a head on collision. During the test, instrumented dummies are placed in the fully belted position to measure the force of impact to the chest, head and leg. The test program deals only with crashworthiness and indicates how well an automobile can protect its occupants in a frontal collision.

There are two types of fixed barrier tests performed to measure the crashworthiness differences of the vehicles [8]. They are full width rigid barrier frontal crash test and offset rigid barrier frontal impact test.

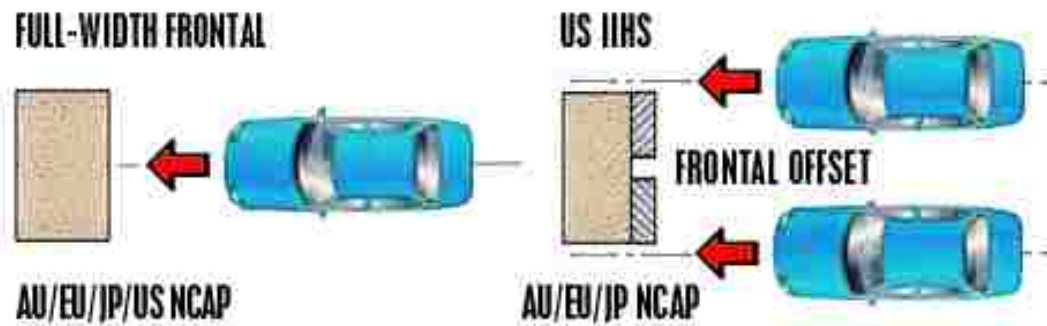


Figure 1.1 Full width and frontal offset crash test [8]

Fixed rigid barrier collisions can represent severe automotive impacts. This test is conducted on automotive vehicles to obtain information of value in reducing occupant injuries and in evaluating structural integrity. The barrier device may be of almost any configuration, such as flat, round, offset, etc. The primary objective of this standard test method is to provide realistic simulation of the forces which act on vehicles and occupants during collisions with fixed objects. Measurements of structural loads and deflections, determination of occupant dynamics, and photographic and post-collision observations of pertinent special events may be useful in establishing design criteria.

Full-width and offset tests complement each other. Crashing the full width of a vehicle into a rigid barrier maximizes energy absorption so that the integrity of the occupant compartment, or safety cage, can be maintained well in all but very high-speed crashes. Full-width rigid-barrier tests produce high occupant compartment decelerations, so they're especially demanding of restraint systems. In offset tests, only one side of a vehicle's front end, not the full width, hits the barrier so that a smaller area of the structure must manage the crash energy. This means the front end on the struck side crushes more than in a full-width test, and intrusion into the occupant compartment is more likely. The bottom line is that full-width tests are especially demanding of restraints but less demanding of structure, while the reverse is true in offsets.

The three factors evaluated in the frontal offset crash test — structural performance, injury measures, and restraints/dummy kinematics — determine each vehicle's overall frontal offset crashworthiness evaluation.

a. Structure/safety cage: Structural performance is based on measurements indicating the amount and pattern of intrusion into the occupant compartment during the offset test. This assessment indicates how well the front-end crush zone managed the crash energy and how well the safety cage limited intrusion into the driver space. Intrusion is measured at 9 places in the driver seating area by comparing the

precrash and postcrash positions of these 9 points. (The steering wheel intrusion is split into upward and rearward components to obtain a total of 10 measurements.) Larger intrusion numbers indicate more collapse of the safety cage.

b. Injury measures: Obtained from a 50th percentile male Hybrid III dummy in the driver seat, injury measures are used to determine the likelihood that a driver would have sustained injury to various body regions. The measures recorded from the head, neck, chest, legs, and feet of the dummy indicate the level of stress/strain on that part of the body. Thus, greater numbers mean bigger stresses/strains and a greater risk of injury.

c. Restraints/dummy kinematics (movement): Significant injury risk can result from undesirable dummy kinematics — for example, partial ejection from the occupant compartment — in the absence of high injury measures. This aspect of performance involves how safety belts, airbags, steering columns, head restraints, and other aspects of restraint systems interact to control dummy movement.

There are different set of rules and test procedures to evaluate the test results for passenger vehicles. Although, there are no well defined set of rules for estimating the crashworthiness of the off-road vehicles, the test methods are evaluated based on the existing rules and procedures.

#### 1.4 Objective of the Research

The goal of the present research was to develop the analysis guidelines for SAE Baja vehicles. The current UNLV Baja frame was analyzed extensively for several worst case load conditions. Modifications to the frame for the improved strength and safety were considered. The analysis recommendations from this work should provide guidelines that will keep the next UNLV team design a more optimized vehicle frame.

Specific objectives were to:

- a) Develop a preliminary design based on specifications given by SAE [1] by meeting the above mentioned requirement and generate the rollcage model in Pro/Engineer Wildfire 4.0.
- b) Perform a linear static analysis that simulates the loads from a frontal impact using FEA techniques. Results of interest from this analysis are Von Mises stress and displacements for different loading conditions on the rollcage structure. The design is aimed for a factor of safety of not less than 1.25. The linear static structural analysis include:
  - i. Grid independence
  - ii. Determining the safe loading conditions
  - iii. Effect of gusset design
  - iv. Other design modifications

- c) Perform the multi body dynamic analysis for the frontal impact crash loading using LS-DYNA to determine acceleration response, energy dissipation during the impact and reaction force on the frame structure.

## CHAPTER 2

### FINITE ELEMENT ANALYSIS

FEA is a powerful design tool that has significantly improved both the standard of engineering designs and the methodology of the design process. The introduction of FEA has substantially decreased the time to take products from concept to the production line. It is primarily through improved initial prototype designs using FEA that testing and development have been accelerated. In summary, benefits of FEA include increased accuracy, enhanced design and better insight into critical design parameters, virtual prototyping, fewer hardware prototypes, a faster and less expensive design cycle, increased productivity, and increased revenue. This section includes FEA tools used in the present research and describes briefly the features and the capabilities of each tool.

#### 2.1 Preprocessor Altair HyperMesh

Altair HyperMesh is a high-performance finite element preprocessor [9] that works with many finite element solvers. It allows engineers to analyze product design performance in a highly interactive and visual environment. HyperMesh's user interface is easy to learn and supports a number of CAD geometry and finite element model file formats, thereby increasing interoperability and efficiency. Advanced functionality within HyperMesh allows the user to efficiently manipulate geometry and mesh

in highly complex models. These functionalities include extensive meshing and model control, morphing technology to update existing meshes to new design proposals and automatic mid-surface generation for complex designs with varying wall thickness. Solid geometry enhances tetra-meshing and hexa-meshing by reducing interactive modeling times, while batch meshing enables large scale meshing of parts with no manual cleanup and minimal user input.

HyperMesh provides direct access to variety of industry leading CAD data formats for generating finite element models. Moreover, HyperMesh has tools to clean up imported geometry containing surfaces with gaps, overlaps and misalignments that prevent high quality mesh generation. By eliminating misalignments and holes, and suppressing boundaries between adjacent surfaces, users can mesh across larger, more logical regions of the model, while improving overall meshing speed and quality. Boundary conditions can be applied to these surfaces for future mapping to underlying future data.

HyperMesh presents users with an advanced suite of easy to use tools to build and edit CAE models. For 2D and 3D model creation, users have access to variety of mesh generation, as well as HyperMesh's powerful auto meshing module. Automatic mid-surface generation, a comprehensive laminate modeler and morphing offer new levels of model manipulation. The surface auto-meshing module in HyperMesh is a tool



for mesh generation that provides users with an ability to interactively adjust a variety of mesh parameters for each surface or surface edge. These parameters include element density, element biasing and mesh algorithm. Element generation can be automatically optimized for a set of user defined quality criteria. User can also employ interactive, process driven tools within HyperMesh for easy model setup, including model assembly using connectors, creation of complex contact definitions, applications of boundary conditions and solver deck preparations.

HyperMesh supports a host of different solver formats for both import and export. Along with fully supported solvers, HyperMesh also provides the flexibility to support additional solvers by way of complete export template language and libraries for the development of input translators. Although HyperMesh support different solvers, in the present application OptiStruct and LS-DYNA solvers are used for static analysis and dynamic analysis respectively to solve the present problem.

## 2.2 Solver OptiStruct

Altair OptiStruct is highly advanced finite-element-based software for both structural analysis and design optimization. OptiStruct is used to design, evaluate and improve performance of mechanical structures. OptiStruct's design module uses the topology optimization approach to generate innovative concept-design proposals. In the initial phase of the development process, the user enters the package space information,

design targets and manufacturing process parameters. OptiStruct generates a design proposal that is optimized for the given design targets.

OptiStruct's analysis module uses the most recent element formulations and a fast, robust sparse-matrix solver for linear static, frequency, buckling or simple contact problems. With its large spectrum of solutions, material models and element types, OptiStruct performs the majority of analysis types for structural analysis, and generates reliable and highly accurate results

Shape optimization is applied on existing product components. OptiStruct's free-shape optimization can be used to reduce high-stress concentrations. OptiStruct can also use HyperMesh's morphing technology to prepare finite element meshes for optimization. As a result, dramatic shape changes are possible without mesh distortion. OptiStruct can easily propose design modifications without underlying CAD data, with minimum user interaction.

OptiStruct is tightly integrated into the HyperWorks environment. Thus, models can be set up completely in HyperMesh. Animations, contour plots and charts can be generated using the post-processing tools in HyperView. OptiStruct uses the NASTRAN syntax to ensure closed-simulation process chains. Moreover, jobs can be easily automated by using a powerful automation and data management layer available in HyperWorks.

### 2.3 Solver LS-DYNA

LS-DYNA is a general purpose explicit and implicit finite element program used to analyze the nonlinear dynamic response of three dimensional structures [10]. Its fully automated contact analysis capability and error checking features have enabled users worldwide to solve successfully many complex crash and forming problems. LS-DYNA is one of the premier software's to study automotive crash and has many default input parameters tailored for crash simulations. For crash simulations, the explicit time integration is used due to advantage over implicit integration method. In the explicit integration method, the solution is advanced without computing the stiffness matrix thus dramatically reducing the time of the simulation. Due to these savings, complex geometries and large deformations can be simulated. LS-DYNA supports a very extensive library of material models. Over one hundred metallic and non metallic material models able to simulate elastic, elasto-plastic, elasto-viscoplastic, Blatzko rubber, foams, glass and composite materials.

LS-DYNA supports a fully automated contact analysis that is simple to use, robust and has been validated. It uses the constraint and penalty method to simulate contact conditions. These methods have been shown to work particularly well in full vehicle crashworthiness studies, systems/component analysis and occupant safety studies. LS-DYNA

supports over twenty-five contact formulations to treat contacts between deformable objects and rigid bodies.

#### 2.4 Post processor Altair HyperView

Altair HyperView is a complete post processing and visualization environment for the finite element analysis, multi body system simulation, digital video and engineering data. HyperView combines advanced animation and XY plotting features with window synchronization to enhance results visualization. Amazingly fast 3D graphics and unparalleled functionality set a new standard for speed and integration of CAE results post processing. HyperView supports many popular CAE solver formats through direct readers, providing flexible and consistent high performance post processing environment.

HyperView's animation client provides a complete suite of interactive post-processing features that dramatically improve results visualization. HyperView also supports an advanced toolset for model query and results comparison for single and overlaid models.

The video client in HyperView introduces the unique capability to read digital video files and synchronize them to CAE animation and XY plot information for enhanced simulation post-processing and correlation. The video client directly reads and writes most standard movie file formats, including AVI, BMP, JPEG, PNG and TIFF. HyperView supports the following:

- i. Multi body dynamics animations with flex-bodies
- ii. Complex animations and complex stress calculations
- iii. Deformed animations
- iv. Linear animations
- v. Transient animations

HyperView's plotting client is a powerful data analysis and plotting tool with interfaces to a wide array of data file formats. Engineers can build, edit and manipulate 2D curves and 3D plots (such as waterfall, surface and 3D line plots) a simple point and click environment provides easy access to curve expressions, axis labels, and legends, plot headers and footers. In addition, plots can be annotated with advanced notes using templates, a built-in text and numeric processor. A sophisticated math engine is capable of processing even the most complex mathematical expressions.

The publishing session export features allows users to output reports to HTML or a power point XML of the active HyperView session. Users can specify which pages are to be written out, as well as specify the format for each window exported.

HyperView supports many popular CAE solver formats through direct readers, providing a flexible and consistent high performance post processing environment. Additional solver formats can be supported through user defined results translator that convert results into the

Altair H3D compressed binary format. This functionality further increases the value proposition of HyperView by broadening its ability to support other commercial and proprietary solver formats.

## CHAPTER 3

### LINEAR STATIC FRONTAL IMPACT ANALYSIS

#### 3.1 Design Methodology

The purpose of this section is to give a basic knowledge of the methodology that was used to analyze the SAE Baja frame member. The Figure 3.1 shows a generic illustration of the major steps involved in the design optimization process.

1. Considering the objectives, functions, design considerations and the rules laid by the SAE Baja, preliminary design of the frame structure was developed.
2. Once the design was established, a CAD model was created using Pro/Engineer Wildfire 4.0 with the preliminary design. The model created was fully parametric to ensure that future changes could be made easily. This model is the basis for creating complex FE model.
3. A finite element (FE) model was created using shell elements using Altair HyperMesh, on which structural analysis was performed. The element quality has been ensured for optimum analysis results.
4. The next step in the analysis was selection of parameters for setting simulation. The parameters include material properties,

section properties, constraints, loading conditions and other simulation related parameters.

5. After setting the parameters, the simulation was run using OptiStruct solver. A static analysis was run for the current problem in the initial stages to find out the optimum parameters for the dynamic analysis.
6. The results of the simulation were interpreted in HyperView. The analysis determines the intensity and the areas of the highest Von Mises stresses and the deformations that the frame members are subjected for the applied loads.
7. If the stresses generated in the chassis member were above the yield limit of the material and/or the deformation of the frame members were more, then existing frame has been modified for the improved performance.
8. The new design has been subjected to the structural analysis with definite input parameters and the process will go on till the stresses and deformation were within the desired limit.
9. Finally, design engineers who consider all manufacturing and cost issues in order to develop a final design should interpret the results of the structural analysis.



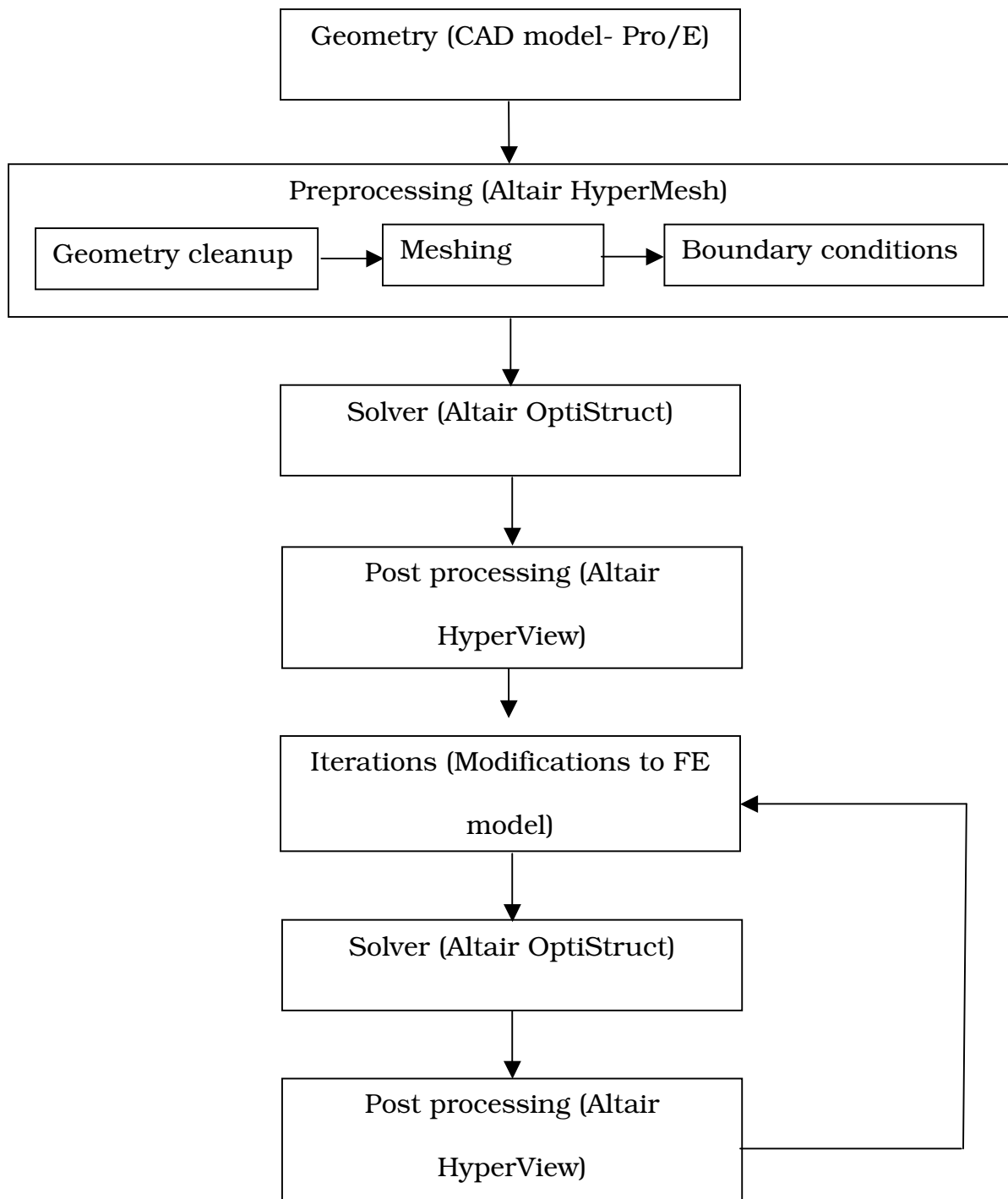


Figure 3.1 Flow chart for generic illustration of design process

### 3.2 Development of a Preliminary Design

The vehicle frame is used to provide a basis on which to mount the various peripherals necessary for self-propulsion. The frame is the “skeleton” of any vehicle. The roll cage provides a framework to protect the operator from hazards and injuries. In the event of a rollover accident, the roll cage is designed to absorb as much of the inertia as possible to lessen the force of the collision on the operator. It means that the chassis was designed to maximize strength and durability, while minimizing weight and retaining manufacturability. It has to support all operator control systems, front and rear suspension systems, and engine and drive train. The objective of the frame design was to satisfy these functions while meeting the SAE regulations with special considerations given to safety of the occupants, ease of manufacturing, cost, quality, weight, and overall attractiveness. Other design factors included durability and maintainability of the frame.

To begin the initial design of the frame, there first must be set some design guidelines. These include not only design features and manufacturing methods, but also the tools to be used in the design. From that point, the areas of the design that may show weakness or high loading should be analyzed for stress concentrations should be identified for analysis.

### 3.2.1 Design Guidelines

Before beginning the design of the frame it was important to make several global design decisions. These include such details as intended steering and suspension design and also intended fabrication methods. While these decisions are not important to the analysis of the frame, they are important to understanding the design. The rules regarding the frame geometry and driver safety must be considered as well.

The intended fabrication is important due to the limitations of the abilities and skills of the build team as well as design directives. The objective is to minimize the number of welded joints on the frame in favor of bent members. Bending is less time consuming and when properly done show a much lower stress concentration. As the design progressed the manufacturability was constantly reviewed with the build team. This ensured that there were no impossible features in the design, and that the team felt confident with its construction. As with the material type, the overall frame geometry is guided by strict rules. These rules were constantly referenced throughout the design of the frame to ensure compliance. As mentioned above the rules change yearly, for this reason they are attached in Appendix A. The interactions of the frame and the strict safety rules required that the frame be designed with a solid modeling software package.

### 3.2.2 The Mini Baja Guidelines

SAE has laid down a set of guidelines and rules that every vehicle should follow. These guidelines are based on recommendations and tests conducted by design professionals. For creating a preliminary design these guidelines were followed to include members in the frame of the chassis. No additional members were added initially, so that the frame with the minimum weight is obtained.

The dimensions of these elements were selected keeping in mind the rules laid down by SAE. No additional members were added. A method of adaptive designing was used wherever possible and considerations were made for the ergonomics of the driver. These members were included in the preliminary design and the minimum possible section was taken i.e. Outer Diameter = 25.4 mm (1.0 in.), Inner Diameter = 19.3 mm (0.76 in.), Material: AISI1020 alloy Steel.

### 3.2.3 Adequate Operator Space

Another objective of the rollcage design is to have adequate operator space for the driver's comfort. The design would allow driver of 1.9 m (6 foot 3 in.) height, 90.7 Kg (200 lbs) weight to fit comfortably into the frame. It was assumed that a driver was placed in the frame in the driving position and measurements were made to make certain all of the SAE safety rules were satisfied.

### 3.3 Geometry Development

A preliminary design was developed by UNLV SAE BAJA team as per the rules and guidelines laid by SAE for the BAJA competition. Since Computer Aided Design (CAD) model is the basis to create a complex FEA model, there began a quest to develop a CAD model. There is no CAD data exists for the preliminary design. To create the CAD, the vehicle was manually measured for the dimensions. With the reference dimensions, a CAD model was developed in Pro/Engineer Wildfire 4.0. CAD drawings were made from the developed model and the frame design was validated to the original dimensions. Figure represents the solid model of the chassis developed in Pro/Engineer wildfire 4.0 for the preliminary design.

Upon completion of CAD model of the frame, the Pro/Engineer part model is imported into the HyperMesh environment which is a part of the Altair HyperWorks software package. Altair HyperMesh was used as the finite element meshing utility in preparation for the optimization study. It is made sure that all the surfaces are imported into HyperMesh properly without any geometry problems. The next step is extracting the mid-surface of the solid pipe model. HyperMesh can automatically generate a mid-surface from a symmetrical cross section. The surface editing tools would allow morphing the generated mid-surface to be convenient for the quadratic meshing. The mid-surface geometry was “cleaned” to prepare

for meshing. This means that some of the lines in the imported model were toggled from edge lines to suppressed (or manifold) lines so that they would not represent an artificial edge that would force the finite elements to unnecessarily align them to. The misreading of lines happens at the locations of fillets and radii features created in CAD models, as the features get falsely interpreted as distinct surfaces in the IGES transformation.

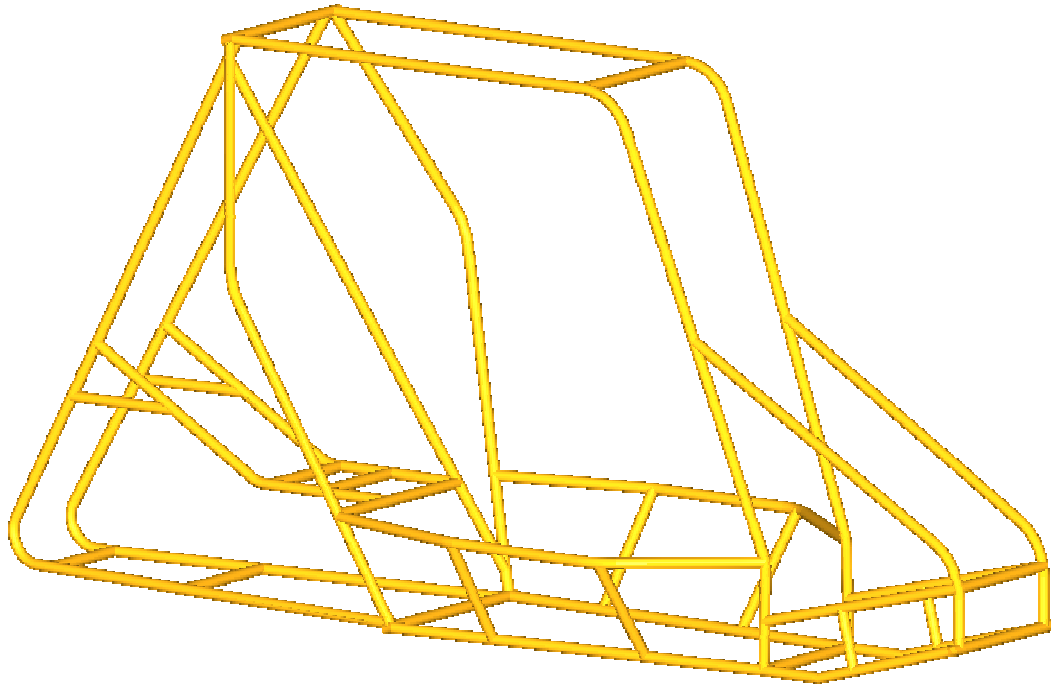


Figure 3.2 Pro/Engineer model for the rollcage frame

Once the geometry was cleaned, the surfaces of the frame member were edited for proper meshing. The surfaces were split at each joint so

that the joints can be meshed first followed by adjacent tube members. In this way mesh quality can be improved. The design space volume was filled with quadrilateral elements using the auto-mesh features of HyperMesh. The mesh size is selected depending upon the requirement. The QI optimization criterion was selected to optimize the mesh quality as per the preset condition. The resulting mesh that was used as the design space for the topology optimization study can be seen in Figures 3.3 & 3.4.

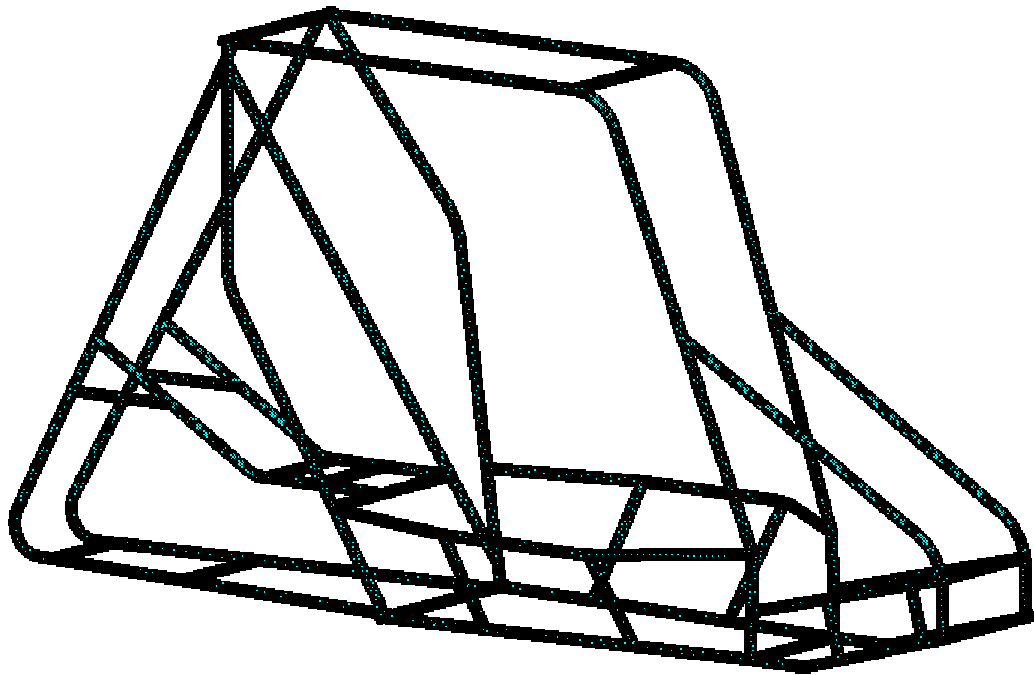


Figure 3.3 HyperMesh model of the rollcage frame member

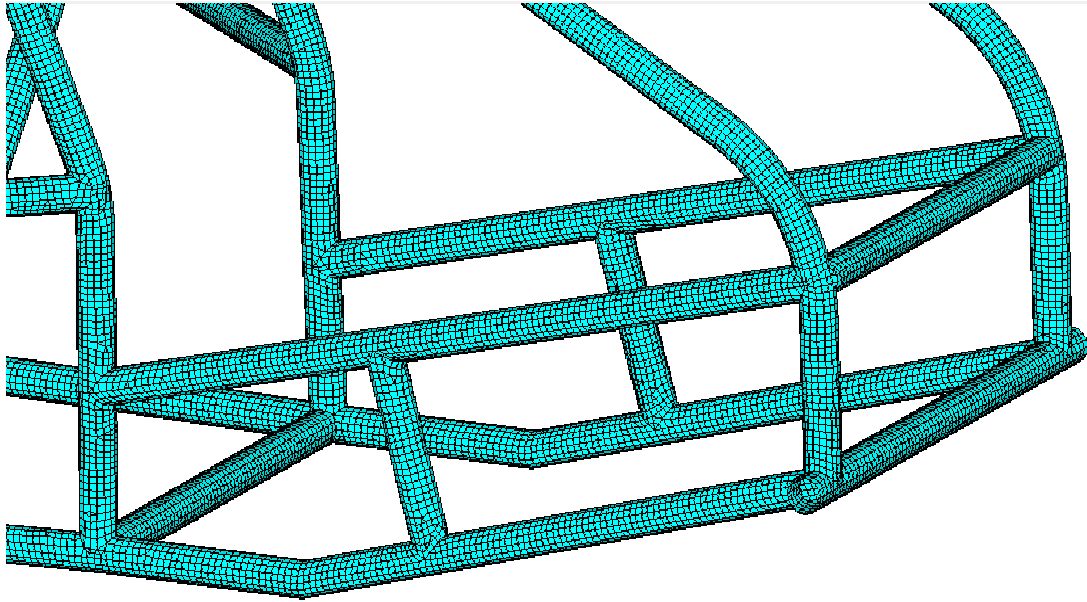


Figure 3.4 Magnified view of the meshed rollcage model

To ensure model accuracy and efficiency, the mesh of the model needs to meet a mesh quality criterion. The quality of the mesh will affect the time step calculations of the simulations and thus the computation time. The time step is directly related to the characteristic length of the elements so the minimum element size is of particular importance. Severely distorted elements will affect the accuracy of the results due to an increase in stiffness of the element due to the distortion. The percentage triangular elements should be less than 5% of the number of elements in the component because the triangular elements impart an artificial stiffness into parts modeled with them. This will cause an



unrealistic behavior of the chassis frame. Figure 3.5 outlines the important mesh quality criteria.

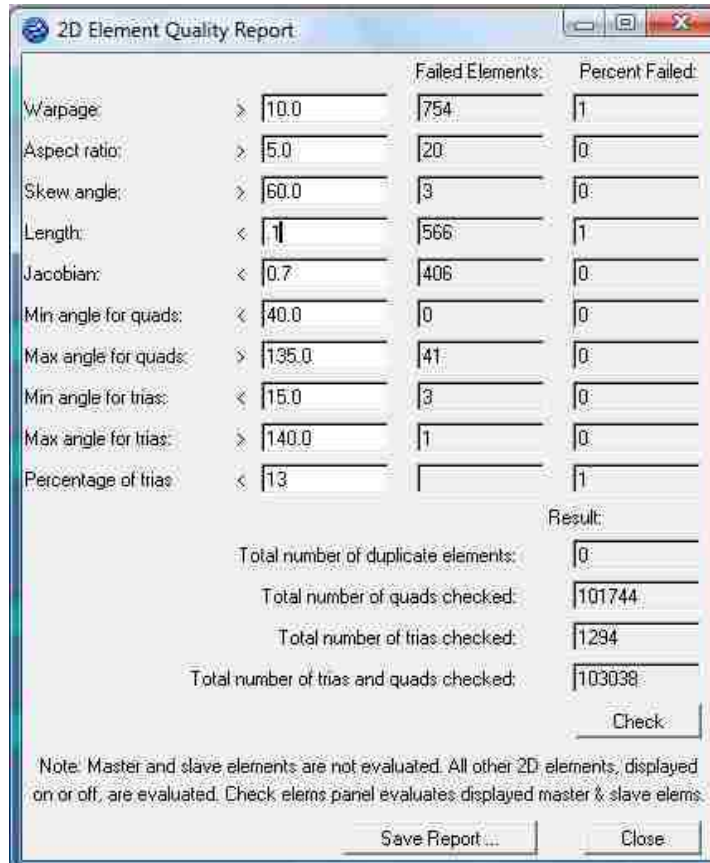


Figure 3.5 2D Element quality report

### 3.4 Material Selection

The materials used in the cage must meet certain requirements of geometry as set by SAE, and other limitations. The main criteria we took into consideration when choosing the material for the roll cage are safety, cost and durability. In a situation where the Baja would roll over, the

material used has to be sturdy enough to protect the driver from fatal injuries. As the frame is used in a racing vehicle, weight is a crucial factor and must be considered. The proper balance of fulfilling the design requirements and minimizing the weight is crucial to a successful design [12].

The rules define the cage to be made with materials equivalent to the following specification [1]:

Steel members with at least equal bending stiffness and bending strength to 1018 steel having a circular cross section having a 25.4 mm (1 inch) OD and a wall thickness of 2.10 mm (0.083 inch)

A key factor of this statement is that only steel members are allowed for the frames construction. However the alloy of the steel is definable as long as it meets the equivalency requirements. These values are required to be calculated about the axis that gives the lowest value. Calculating the strength and stiffness this way ensures that tubes with a non-circular cross-section will be equivalent even in a worst case loading situation. The rules go on further to define bending strength and stiffness by:

Bending stiffness is proportional by the EI product and

Bending strength is given by the value of  $S_y I/c$ ,

(For 1018 steel the values are;  $S_y = 370 \text{ MPa (53.7 ksi)}$   $E = 205 \text{ GPa (29,700 ksi)}$ )

$E$  = Modulus of elasticity

$I$  = Second moment of area for the cross section about the axis giving the lowest value

$S_y$  = Yield strength of material in units of force per unit area

$c$  = Distance from the neutral axis to the extreme fiber

While the rules set many factors of the material's geometry there are other limitations. These limitations include the method of fabrication and industry standards for the material. The frame will be built using a bent tube construction and TIG welded joints. The geometry is limited by industry standards. It is important to utilize commonly available tubing sizes and materials. By considering all the above factors, AISI 1020 graded steel is considered for the frame material. The material and section properties of AISI 1020 steel are given in table 3.1.

### 3.5 Linear Static Frontal Impact Analysis

Linear static analysis is carried out on the chassis to test different loading conditions and to find out the resulting stresses and deformation on the frame members. Knowing how the current design reacts to different loading conditions would allow designers to make changes prior to physical prototyping. In addition, a linear static analysis is a base for dynamic or non-linear FEA analysis. If a design cannot survive a linear static stress analysis it has to be fixed before moving on to more complex, time consuming and expensive dynamic or non-linear analysis.

Table 3.1 Material Property of the Frame [6]

S.NO	PROPERTY	VALUE
1	Material (Steel)	AISI 1020
2	Outer Dia (mm)	25.4
3	Inner Dia (mm)	19.3
4	Section Thickness (mm)	3
5	Area moment of Inertia (mm <sup>4</sup> )	8324.6
6	Young's Modulus E (MPa)	247,749
7	Yield Strength Sy (MPa)	594.6
8	Density (Kg/m <sup>3</sup> )	7861
9	Poisson Ratio	0.3

The next stage in the design process is to perform a finite element linear static stress analysis, review the stress and deformation pattern on the frame members and modify the frame members to reduce the stress and deformation so as to withstand the applied load. Although, a vehicle needs different types of FE analysis to validate its design, for the current problem a frontal impact analysis is carried out to study the effect of loading on the frame.

Assumptions for frontal impact simulation:

1. The chassis material is considered isotropic and homogeneous

2. Chassis tube joints are assumed to be perfect joints
3. The impact barrier is not deformable.

### 3.5.1 Loading / Boundary Conditions

Frontal impact is a dynamic event but it is easier to do preliminary analysis using linear elastic quasi-static analysis. Therefore we need to determine a force value to use in the static analysis that is roughly equivalent to the peak dynamic force or average dynamic force observed during an impact. One way to estimate a maximum allowable force is to start with a simplified injury criterion. Research has found that the human body will pass out at loads much higher than 9 times the force of gravity or 9 G's. A value of 10 G's was set as the goal point for an extreme worst case collision [13]. For the static frontal impact analysis, a deceleration of 10 G's was assumed for the loading which is equivalent to a static force of 26,698 N (equivalent to 6000 lbf) load on the vehicle, assuming the weight of the vehicle is 272.16 Kg (600 lbs).

Florida Institute of technology SAE Baja team analyzed the data from 'The motor Insurance Repair Research Center' and estimated the maximum g-force that the Baja car will see is 7.9 G's [14, 15]. To calculate the forces used to analyze the 7.9 G impact, Newton's second law was used. The force calculation was shown below in equation.

$$F = ma$$

$$m = 272.16 \text{ Kg (600 lbs)}$$

$$a = 7.9 \times 9.81 \text{ m/s} = 77.5 \text{ m/s}$$

$$F = 272.16 \times 77.5 = 21,092.4 \text{ N (equivalent to 4750 lbf)}$$

### 3.5.2 Analytical Calculation for Impact Force

The vehicle for SAE BAJA is designed for a maximum speed of 17.88 m/s (40mph) for the competition [15]. The total weight of the vehicle including the driver is estimated to be 272.16 kg (600 lbs).

For a perfectly inelastic collision, the impact force can be estimated using the below equation:

$$W_{net} = \frac{1}{2}mv_{final}^2 - \frac{1}{2}mv_{initial}^2$$
$$W_{net} = f \times d$$

This equation states that the change in kinetic energy is equal to the net work done, and the work needed to stop the car is equal to the force times the distance.

$$f \times d = -\frac{1}{2}mv_{initial}^2$$

It is considered for the static analysis that the vehicle comes to rest 0.1 sec after the impact [16]. For a 17.88 m/s (40 mph) speed, the travel of the vehicle after the impact is 1.79 m.

$$\text{Impact force} = \frac{1}{2} * 272.16 * 17.88^2 * \frac{1}{1.79} = 24,304 \text{ N}$$

The frame does not need to survive the crash load so long as it protects the driver in this situation. Here, we have three different types of loads i.e. 26,698 N (10G force), 21,092 N (7.9G force) & 24,304 N (analytical value). In the initial stages, the current frame design is aimed to withstand the impact load of 33,262 N (7500 lbf). If not, it is made sure that the frame withstands an impact load of 26,698 N (equivalent to 6000 lbf) minimum, with a design factor of safety of 1.25.

The finite element analysis software program used for solving the problem for structural kinematics analysis was Altair OptiStruct. The frontal impact analysis was run for different grid sizes and the effect of Von Mises stress and displacement was reviewed for each case for the chassis members. Changes or modifications were done accordingly to the chassis members to withstand the impact load (i.e. Generated Von Mises stress should be less than the yield stress of the material).

## CHAPTER 4

### RESULTS & DISCUSSION FOR THE STATIC ANALYSIS

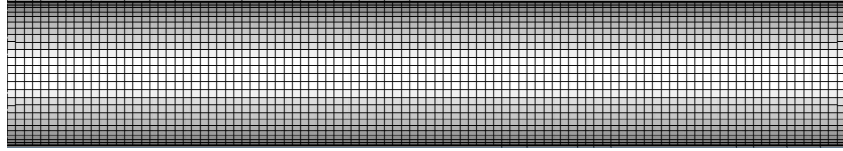
#### 4.1 Grid Independence

Mesh size is an important parameter to consider in a numerical analysis due to artificially defining a distribution of displacement or stress in the elements, whether the modeling is based on a continuum or a discontinuum approach. Grid size or mesh size plays an important role in both convergence and accuracy of the solution. Theoretically, a computational model with a finer mesh size obtains a more accurate result. Though, the use of high-density mesh improves the accuracy of simulation, but is computationally expensive and at times the solution may be impossible. On the other hand, too fine mesh may not produce more accurate results, because other factors such as time step and boundary condition may govern the modeling accuracy. A course mesh is used to quickly examine the solver settings and boundary conditions. This means that the numerical model with coarse mesh will take less time for computation than the fine mesh. Hence, grid independence studies are performed to obtain an optimized mesh size.

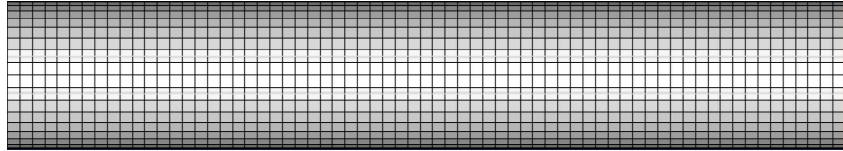
Grid independency is the non-variation of the results with change in the grid density. It is performed to make sure that the ideal grid size is used during the computation process, which avoids the unnecessary computational space and time. It is one way to make the best use of



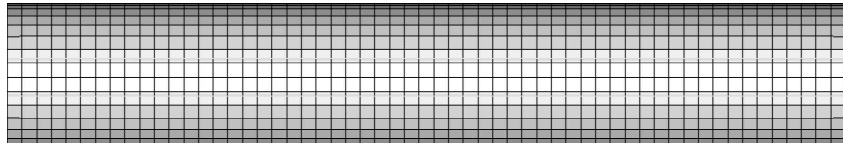
available resources economically. For the current problem, grid independency was accomplished by simulating the frontal impact analysis for various grid/mesh sizes. The results obtained from each grid size are compared. Initially a coarse mesh with size 5.08 mm (0.2 in.) is used to study the effects of the frontal impact on the SAE Baja chassis frame. The mesh size was reduced for the further analysis to 4.57 mm (0.18 in.), 4.24 mm (0.167 in.), 3.6 mm (0.14 in.), 3.05 mm (0.12 in.), 2.54 mm (0.10 in.), 2.23 mm (0.088 in.), 1.9 mm (0.075 in.) and 1.27 mm (0.05 in.) subsequently the numbers of elements are increased. For each case, the analysis for frontal impact is run and the values of the maximum stress and displacement after the impact are listed. The mesh size is stable or the grid independency is reached if the stress and deflection of the frame after impact is less than 10% for various grid sizes Figure 4.1 represents the mesh configuration of similar pipe with various grid sizes.



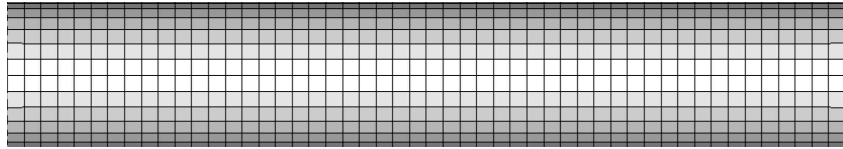
Mesh Size: 1.27 mm (0.05 in.)



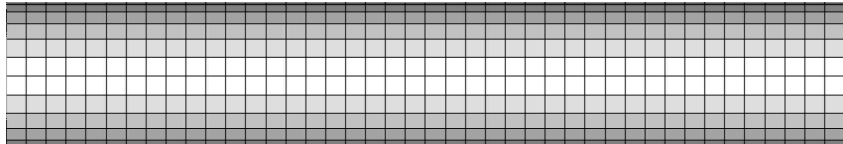
Mesh Size: 1.9 mm (0.075 in.)



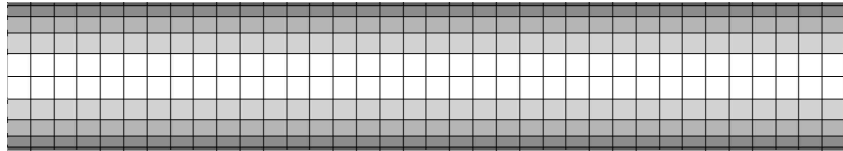
Mesh Size: 2.23 mm (0.088 in.)



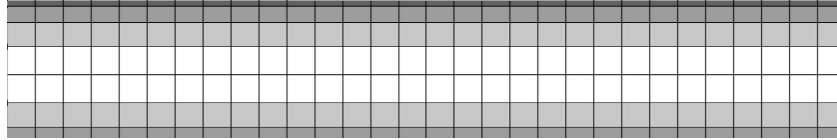
Mesh Size: 2.54 mm (0.1 in.)



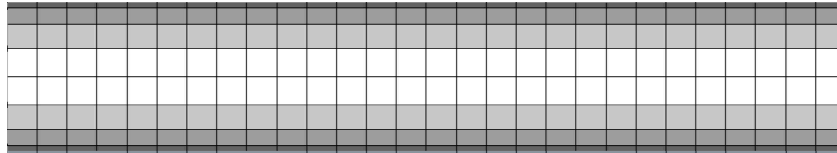
Mesh Size: 3.048 mm (0.12 in.)



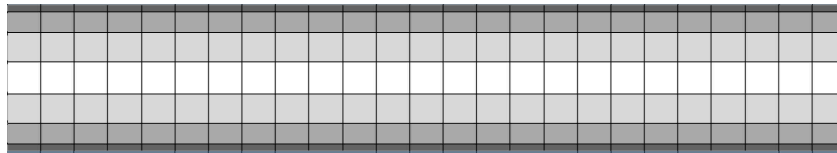
Mesh Size: 3.56 mm (0.14 in.)



Mesh Size: 4.24 mm (0.167 in.)



Mesh Size: 4.57 mm (0.18 in.)



Mesh Size: 5.08 mm (0.2 in.)

Figure 4.1 Mesh configuration for various grid sizes

Table 4.1 represents the effect of the maximum Von Mises stress and the displacement on mesh size. It can be observed from the results that the maximum stress increases with the decrease of the grid size. The deflection of the frame after impact is less than 10% for various grid sizes and is assumed to be independent of the grid size. It can be conferred from the results that the convergence stress is the main criteria for selecting the grid size rather than the deflection.

Table 4.1 Effect of maximum stress and displacement on mesh size

S. No	Mesh Size (mm)	No. of Elements	No. of DOF	Max. Von Mises Stress (MPa)	Max. Displacement (mm)
1	1.27	597,443 (Localized mesh refinement)	3,561,360	2192.53	21.54
2	1.91	507,408	3,030,570	1751.27	21.89
3	2.24	385,244	2,299,686	1503.06	22.81
4	2.54	294,141	1,762,104	1337.58	21.79
5	3.05	210,290	1,258,626	1054.90	21.16
6	3.56	151,870	904,548	1020.42	21.69
7	4.24	103,134	613,647	958.37	25.10
8	4.57	94,286	560,526	917.00	22.40
9	5.08	75,071	448,404	848.06	23.06

The maximum stress does not occur at same locations for all the simulations. For most of the analyses, the location of the maximum stress is either on the left or the right constraint as represented in the

Figure 4.2. For mesh size 4.24 mm the location of the maximum stress is at the front bumper. Since the maximum stress is not at the same location for all the cases, it is unfair to conclude the grid size for the independence based on the max stress convergence. In order to accurately test the grid independency, the behavior of the frame for stress and deflection at different locations to be studied for various mesh sizes.

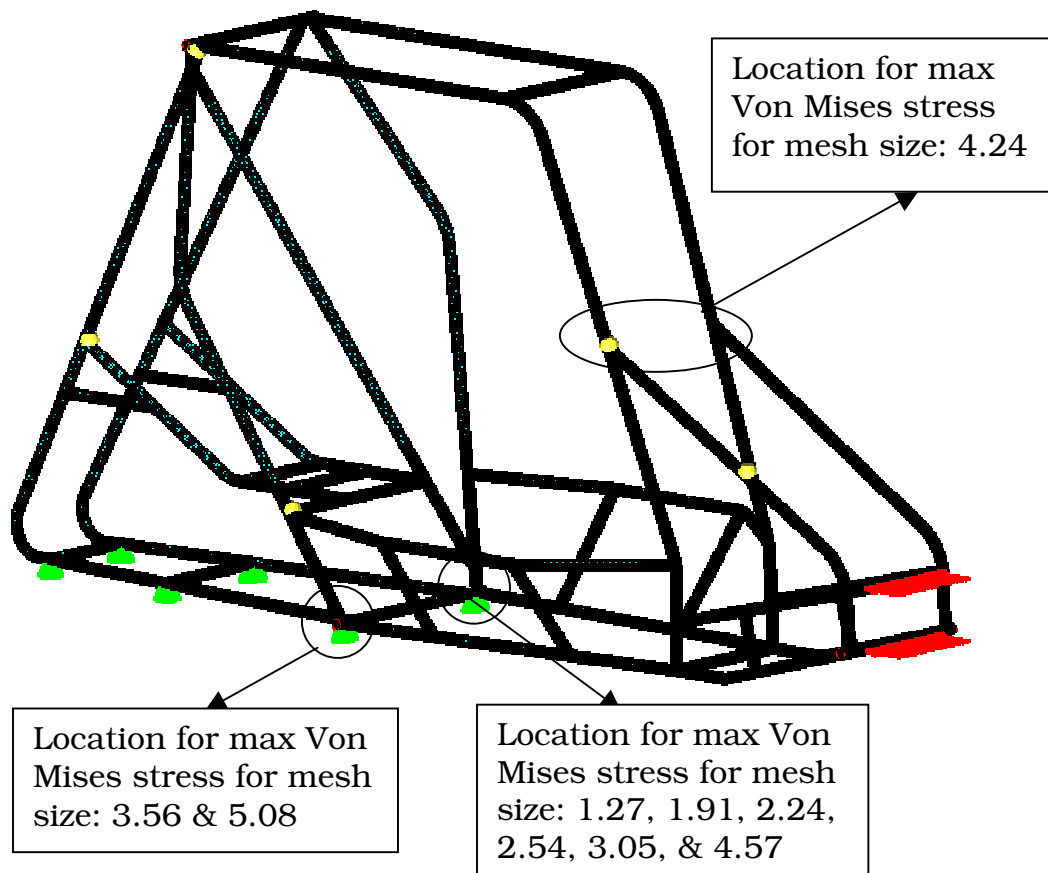


Figure 4.2 Location of maximum Von Mises stress for various mesh sizes

The Von Mises stress and the deflection for five selected point locations are shown in Table 4.2 and 4.3. The results are plotted for the analysis as shown in Figures 4.2 & 4.3. The point locations, as shown in Figure 4.5 are selected to find out the exact behavior of the frame for stress and deflection at the joints and the middle of the frame on front and back of the chassis for various mesh sizes. It can be observed from the results that the Von Mises stress decreases with the increase of the mesh size at all selected locations as shown in Figures 4.6 & 4.7. The deflection after impact does not influence much on the mesh size. The table indicates that the variation of the displacement after the loading is less than 10% for the different grid sizes.

The FEA model was said to achieve grid independent when the solutions from two grid sizes are within predetermined tolerance limits. For the same location the maximum percentage difference in the Von Mises stress values were observed to be less than 10% for all given mesh sizes. So it is decided to select the grid size based on the maximum values of stress since the variation of displacement at different points B, C, D & E for all mesh sizes are almost uniform. In addition, the mesh size for the grid independence should be selected based on the computational time and the memory requirement for solving the problem.

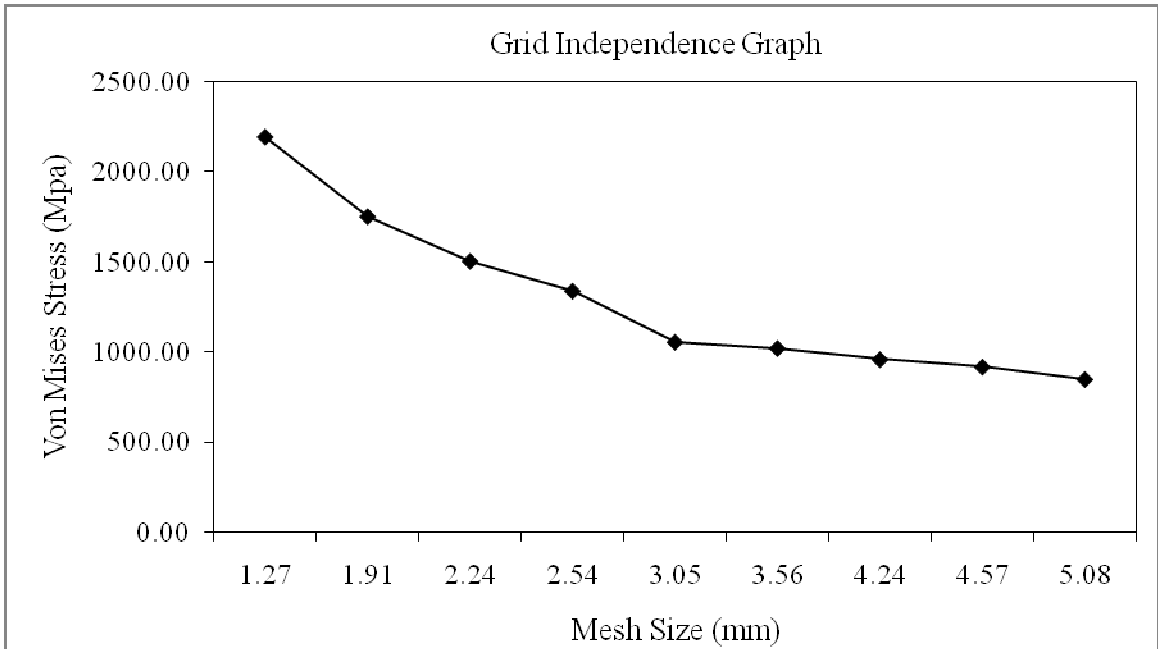


Figure 4.3 Grid independence study graph for the max Von Mises stress

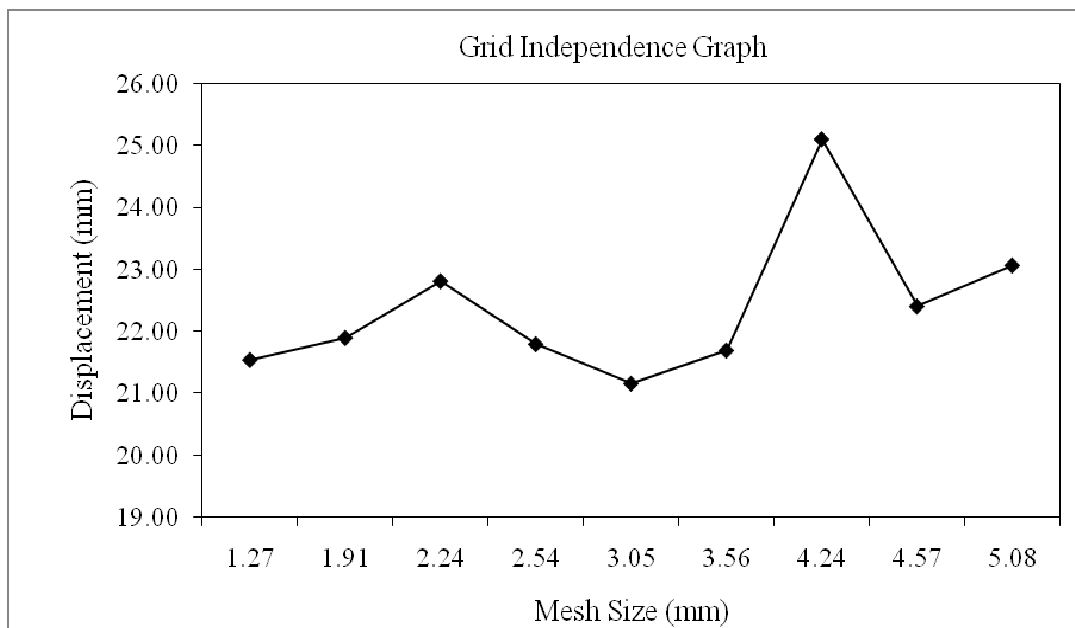


Figure 4.4 Grid independence study graph for the max displacement

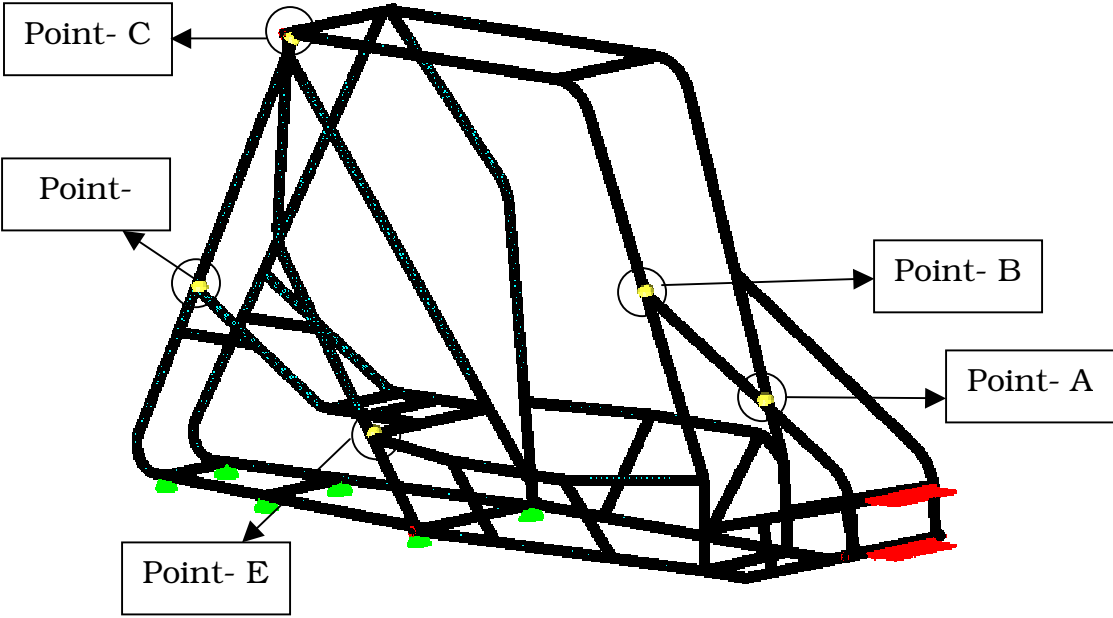


Figure 4.5 Selected locations of the points



Table 4.2 Von Mises stress at selected locations after the impact loading

S. No	Mesh Size (mm)	Von Mises Stress (MPa)				
		Point -A	Point - B	Point - C	Point - D	Point - E
1	1.27	--	965.27	747.39	342.05	36.75
2	1.91	14.46	917.69	739.12	327.43	39.92
3	2.24	18.42	910.11	698.44	333.22	40.20
4	2.54	17.68	901.83	658.59	318.12	38.33
5	3.05	13.95	823.92	685.13	299.58	37.51
6	3.56	15.39	774.28	617.22	295.03	39.09
7	4.24	17.35	905.28	568.68	314.06	42.09
8	4.57	16.49	790.83	597.78	296.06	36.34
9	5.08	16.02	704.64	591.78	272.21	39.33

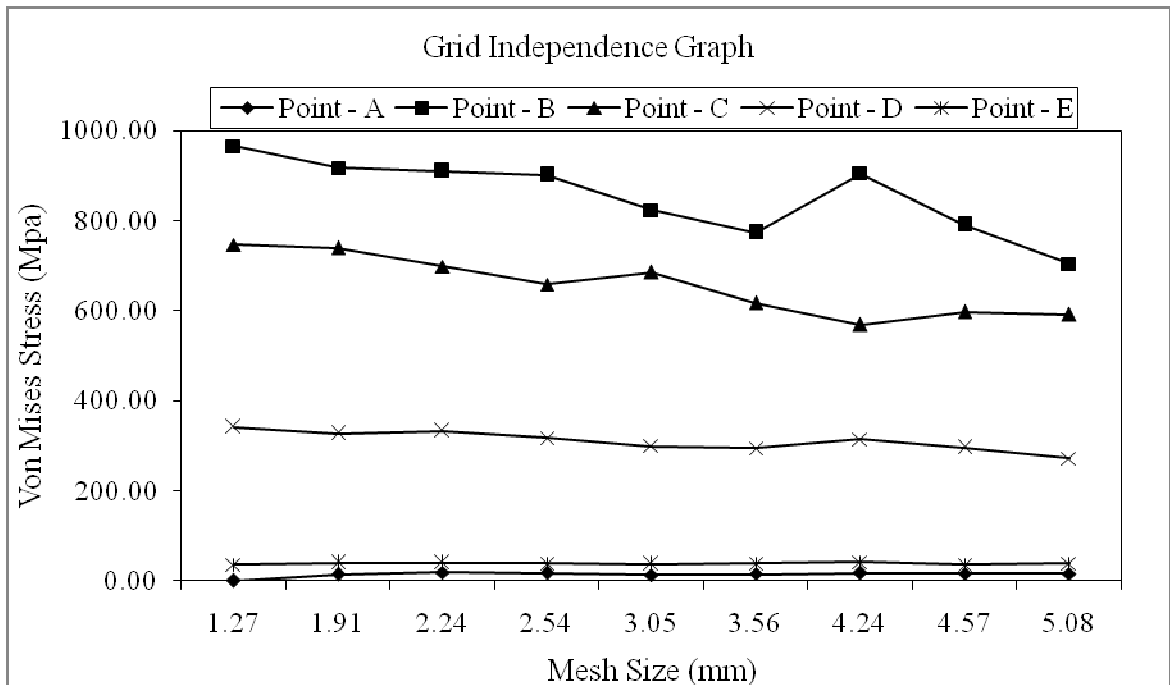


Figure 4.6 Grid independence study graph for stress at selected locations

Table 4.3 Displacement of the frame at selected locations after the impact

S. No	Mesh Size (mm)	Displacement (mm)			
		Point - B	Point - C	Point - D	Point - E
1	1.27	16.22	6.81	2.49	2.62
2	1.91	16.31	6.83	2.56	2.61
3	2.24	16.76	7.13	2.66	2.75
4	2.54	16.36	6.91	2.56	2.64
5	3.05	15.90	6.72	2.46	2.51
6	3.56	16.27	6.77	2.44	2.53
7	4.24	18.80	7.83	2.90	2.98
8	4.57	16.82	7.05	2.58	2.66
9	5.08	17.19	7.22	2.67	2.78

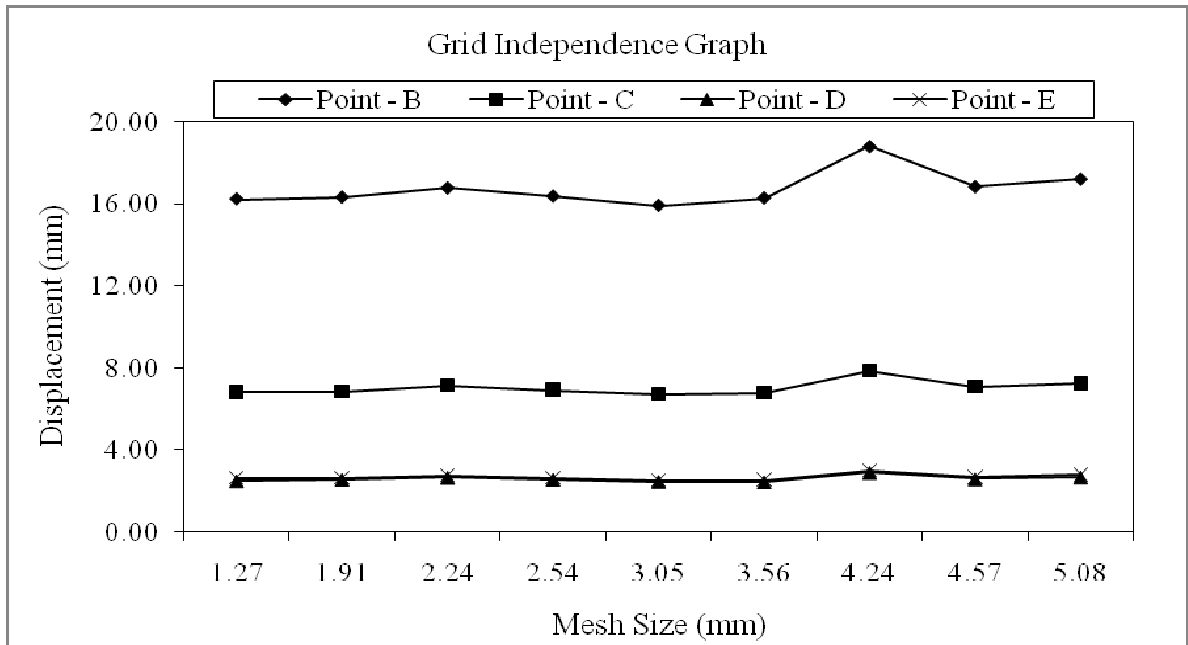


Figure 4.7 Grid independence study graph for displacement at selected locations

Table 4.4 Effect of the mesh size on computation time & memory

S. No	Mesh Size (mm)	No. of Elements	No. of DOF	Computation Time (Min)	Memory to run the simulation (MB)
1	1.27	597,443	3,561,360	108.85	1541
2	1.91	507,408	3,030,570	59.33	1312
3	2.24	385,244	2,299,686	235.1*	1237
4	2.54	294,141	1,762,104	22.5	948
5	3.05	210,290	1,258,626	147*	679
6	3.56	151,870	904,548	5.88	488
7	4.24	103,134	613,647	2.25	331
8	4.57	94,286	560,526	2.75	304
9	5.08	75,071	448,404	2.3	244

\*Analysis run on different server

In general, refining the mesh by a factor of 2 can lead to a 4-fold increase in problem size. The increase in the problem size increases the degrees of freedom which in turn increase the computation time. This is

clearly unacceptable for a piece of software intended to be used as an engineering design tool operating to tight production deadlines. The more number of DOF, the more is the memory required to solve the problem and save the results. In some cases, the increase in the number of elements may cause the meshing problems. Table 4.4 represents the computation time and the memory required to solve the problem. In the present case, mesh size of 1.27 mm has caused great meshing problems. So instead of meshing uniformly with 1.27 mm all over, the joint areas were meshed with the required length of 1.27 mm and the remaining areas equivalences with appropriate mesh size. From the following table, it can be concluded that the memory requirement and computation time for mesh size 4.24 mm are optimal for the current problem.

It could be concluded from the above graphs and tables for Von Mises stress, displacement and computation time and memory requirements that 4.24 mm mesh size is optimum for grid independence for the SAE Baja vehicle with the current design.

## 4.2 Strengthening Mechanism

In an attempt to alleviate stress concentrations resulting from chassis geometry as well as improve the frame's torsional stiffness, strengthening mechanisms like gusseting at the nodes were incorporated into the design.

#### 4.2.1 Providing gussets at the critical joints of the frame

It is observed from the results that the stress concentration is more at the joints of the frame members. In order to reduce the effects of stress concentration so as to avoid the catastrophic failure of the frame under loading or impact, gussets are provided at the area of high stress concentration [17]. Gussets are pieces of sheet steel that are welded tangential to the two tubes intersecting at a node. They reduce the stress concentration by distributing the force of impact further down the intersecting members. The primary purpose of the gussets was to increase the rollage safety factor and provide better protection for the driver in a roll over a scenario. They also help to increase the overall frame stiffness which will benefit vehicle control and feel during normal or bumpy driving conditions. Although there are different gusset shapes available, in the present analysis only triangular shaped gussets are used. Even though it is not mentioned in the report, addition of a relief hole at the center of the gusset would effectively reduce the weight without effecting the stress concentration. Figure 4.8 clearly depicts the addition of the gussets to the roll-cage.

The stress concentration depends on the size (length & height) and slenderness ratio (ratio of length to thickness) of the gusset. Here an attempt has been done to find out the optimum size and design of the gusset for the current frame member.

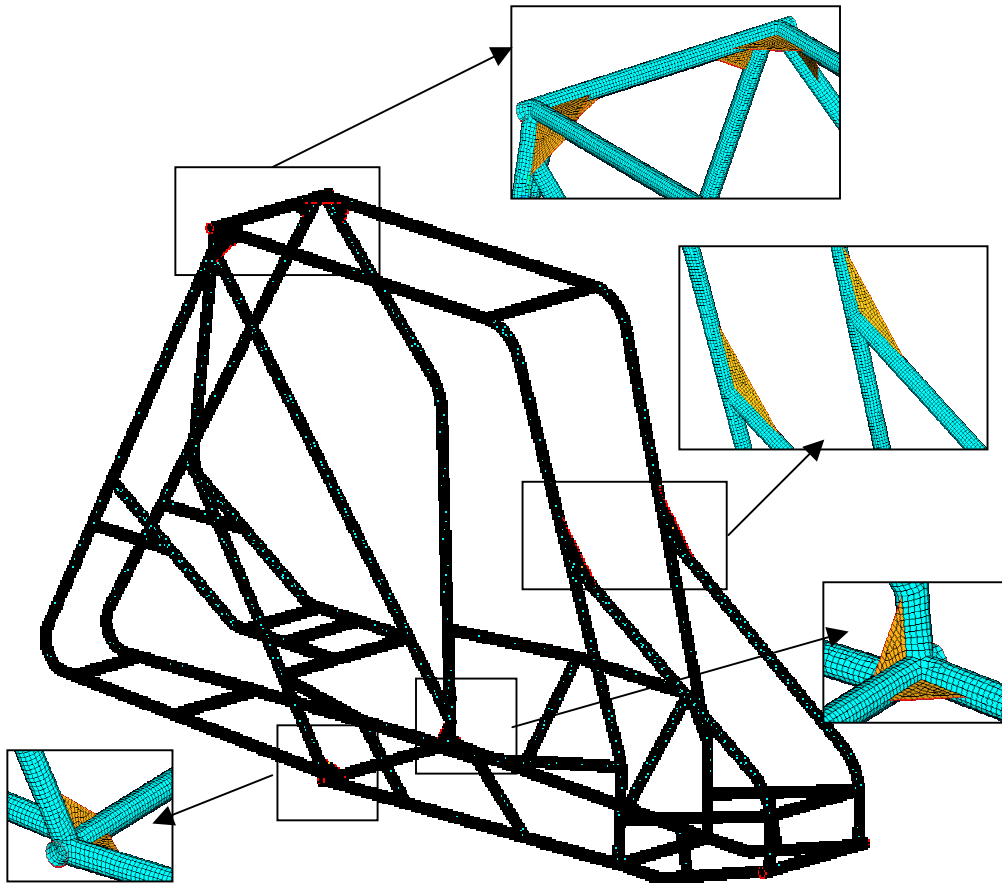


Figure 4.8 Provision of gussets at the frame joints

#### 4.2.2 Effect of gusset size on stress concentration

Frontal impact analysis is carried out for different sizes (length, width and thickness) of gusset. The effect of max Von Mises stress and the max displacement on the frame member is studied for various gusset sizes. Table 4.5 represents the effect of gusset size on the maximum Von Mises stress of the frame. It is observed from the results that provision of

gusset would reduce the maximum stress by 17-21 %. The lowest Von Mises stress now is 751.53 MPa for gusset size of 88.9 mm L x 88.9 mm H x 6.35 mm T (3.5 in. L x 3.5 in. H x 0.25 in. T). It is also observed from the Figure 4.9 that with the increase in gusset thickness, the maximum Von Mises stress decreases and similarly with the increase of gusset size per side (length and width) the maximum stress also reduces. In actual case, the gussets are to be welded over the pipe of outer diameter 25.4 mm. The maximum thickness of the gusset for the analysis is set based on the feasibility of welding the gusset of the curvature of the pipe. Based on this criterion, the maximum limit for the thickness is set as 6.35 mm.

Table 4.6 represents the effect of gusset size on the maximum displacement of the frame. It is observed that provision of gusset would reduce the maximum displacement by 11-17%. The lowest displacement with gusset is 5.62 mm, for gusset size of 88.9 mm L x 88.9 mm H x 6.35 mm T, which is the same for the lowest Von Mises stress with the gusset. It is also observed from the Figure 4.10 that with the increase in gusset thickness, the maximum displacement decreases and similarly with the increase of gusset size per side (length and width) the maximum displacement also reduces.

So it can be concluded from the above results that the optimum gusset size is 88.9 mm L x 88.9 mm H x 6.35 mm T for the chassis frame member.

Table 4.5 Effect of gusset size on the max. Von Mises stress of the frame

S.No	Size of the Gusset (mm)		Max. Von Mises stress (Mpa)		% Change in the stress
	Length per side	Thickness	With gusset	Without gusset	
1	88.90	3.18	786.00	958.37	17.99
2		3.81	779.11	958.37	18.71
3		4.45	765.32	958.37	20.14
4		5.08	758.42	958.37	20.86
5		5.72	758.42	958.37	20.86
6		6.35	751.53	958.37	21.58
7	76.20	3.18	792.90	958.37	17.27
8		3.81	786.00	958.37	17.99
9		4.45	779.11	958.37	18.71
10		5.08	772.21	958.37	19.42
11		5.72	765.32	958.37	20.14
12		6.35	758.42	958.37	20.86
13	63.50	3.18	799.79	958.37	16.55
14		3.81	792.90	958.37	17.27
15		4.45	786.00	958.37	17.99
16		5.08	779.11	958.37	18.71
17		5.72	772.21	958.37	19.42
18		6.35	765.32	958.37	20.14



Table 4.6 Effect of gusset size on the max. Displacement of the frame

S.No	Size of the Gusset (mm)		Max. Displacement (mm)		% Change in the stress
	Length per side	Thickness	With gusset	Without gusset	
1	88.90	3.18	5.79	6.81	14.98
2		3.81	5.74	6.81	15.69
3		4.45	5.71	6.81	16.19
4		5.08	5.67	6.81	16.70
5		5.72	5.65	6.81	17.11
6		6.35	5.62	6.81	17.51
7	76.20	3.18	5.91	6.81	13.26
8		3.81	5.87	6.81	13.87
9		4.45	5.83	6.81	14.37
10		5.08	5.80	6.81	14.88
11		5.72	5.77	6.81	15.28
12		6.35	5.75	6.81	15.59
13	63.50	3.18	6.03	6.81	11.54
14		3.81	5.99	6.81	12.04
15		4.45	5.96	6.81	12.55
16		5.08	6.03	6.81	11.44
17		5.72	5.90	6.81	13.36
18		6.35	5.88	6.81	13.66

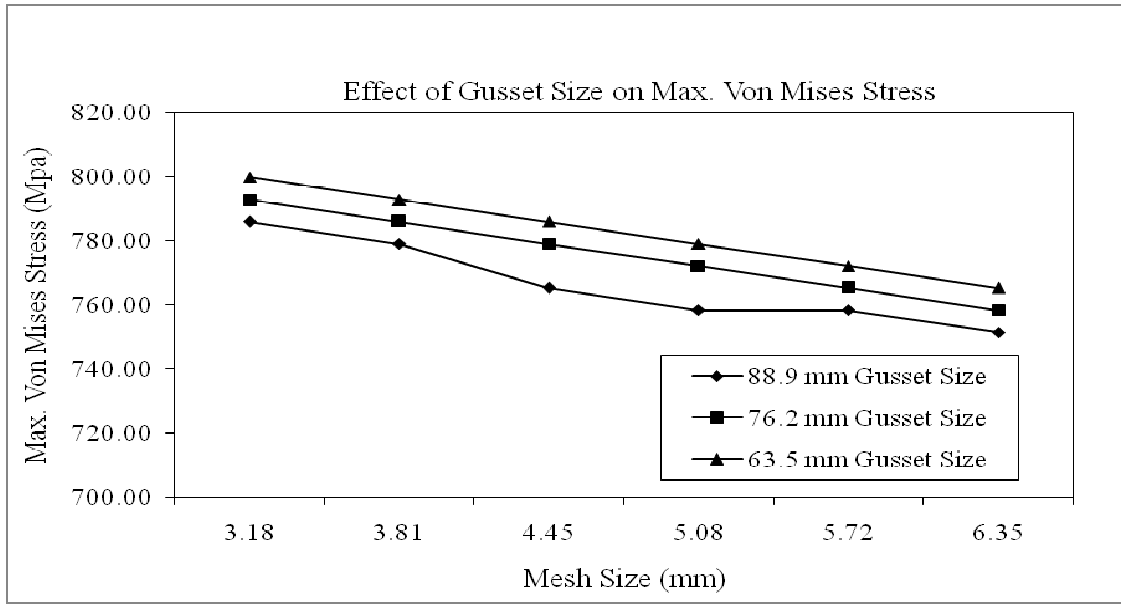


Figure 4.9 Effect of gusset size on the max Von Mises stress of the frame

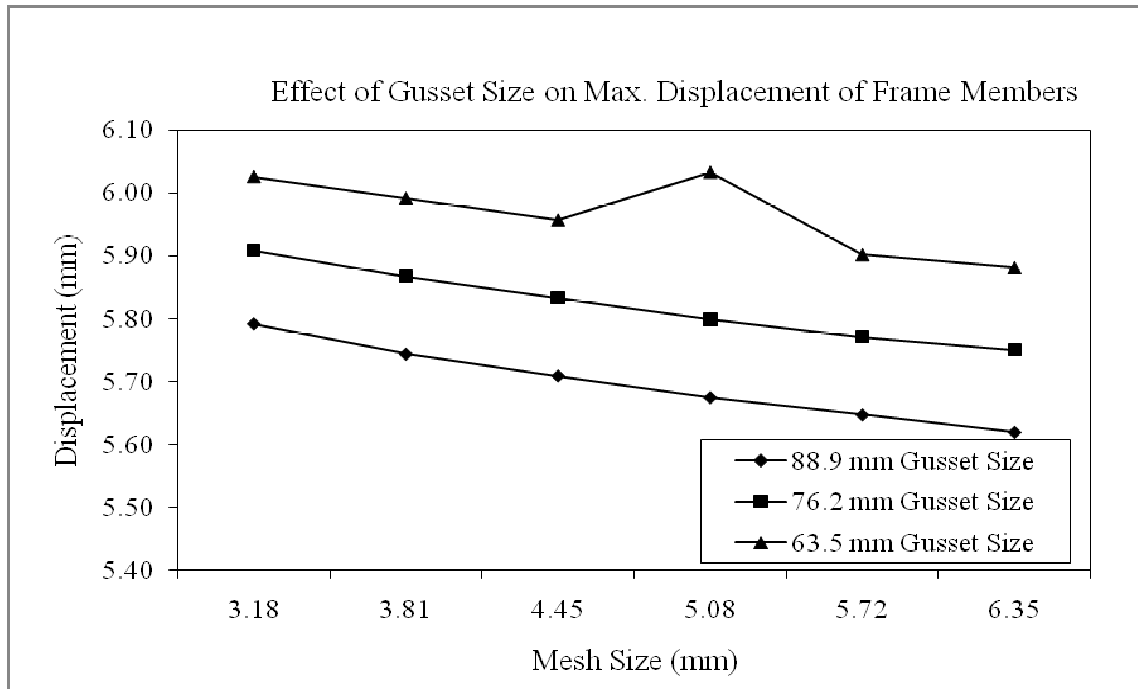


Figure 4.10 Effect of gusset size on the max. Displacement of the frame

### 4.3 Load carrying capacity of the frame

The maximum Von Mises stress generated in the chassis frame for 33,362 N (7500 lbf) load condition is relatively higher. The stress in every case for the same loading condition is more than the yield stress of the material. This signifies that the material of the chassis frame could not be able to withstand the generated forces due to impact. Since the frame is already manufactured or welded with this design, UNLV SAE team is intended to use the frame for the competition this year with slight changes in the design. In this research, an attempt has been made to find out the load carrying capability of the frame member.

The OptiStruct analysis is carried out for the gusset frame design for different loading conditions. The static load is varied to 33,362 N (7500 lbf), 31,138 N (7000 lbf), 28,913 N (6500 lbf), 26,689 N (6000 lbf), 24,465 N (5500 lbf) and 22,241 N (5000 lbf) for the frontal impact analysis. Table 4.7 shows the effect of different loads on the Von Mises stress and displacement of the frame members.

Figures 4.11 and 4.12 represent the variation of the Von Mises stress and displacement with the impact loading. The yield stress for the frame material is 594.6 MPa (86,240 psi) and any stress beyond that would be undesirable for the designer point of view. The Von Mises stress for 33,362 N static load is 751.53 MPa which is above the yield stress of the frame material. The static load is reduced to 31138 N the stress induced

in the member is 533.64 MPa which is below the yield stress and is considered to be safe load for the frame. The maximum displacement for the above load is reduced drastically from 21.16 mm to 2.59 mm.

Table 4.7 Effect of impact load on Von Mises stress and displacement

S.No	Grid Size (mm)	Gusset Size (LxHxT) (mm)	Static Load (N)	Von Mises Stress (MPa)	Displacement (mm)
1	4.24	88.9 x 88.9 x 6.35	33362	751.53	21.16
2	4.24	88.9 x 88.9 x 6.35	31138	533.65	3.51
3	4.24	88.9 x 88.9 x 6.35	28913	504.01	3.28
4	4.24	88.9 x 88.9 x 6.35	26689	472.29	3.05
5	4.24	88.9 x 88.9 x 6.35	24465	453.68	2.84
6	4.24	88.9 x 88.9 x 6.35	22241	447.47	2.59

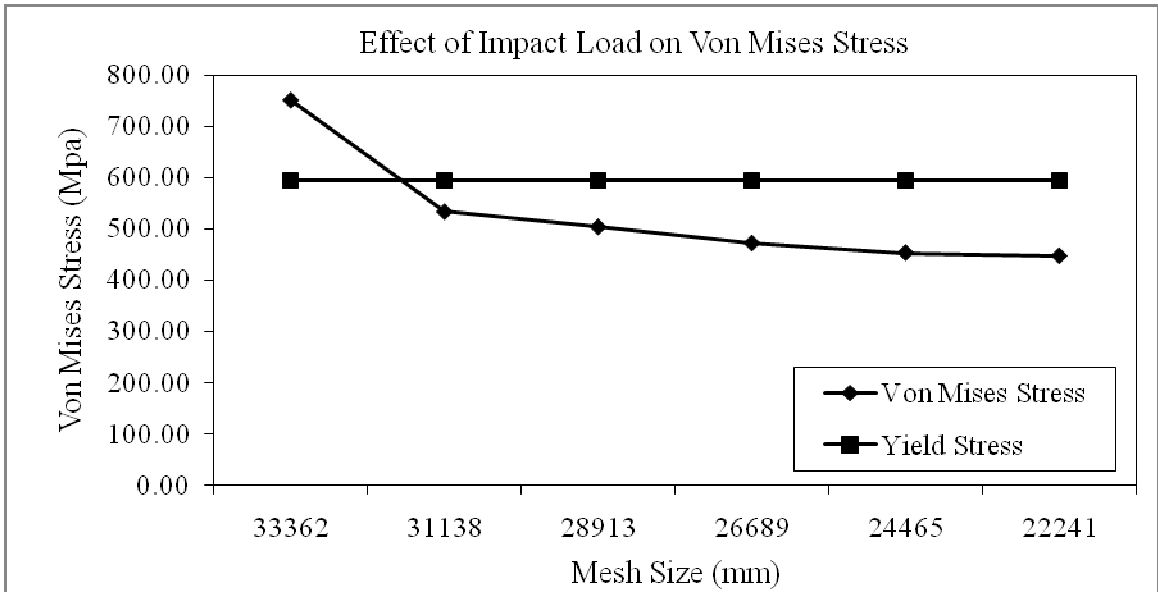


Figure 4.11 Effect of impact load on maximum Von Mises stress

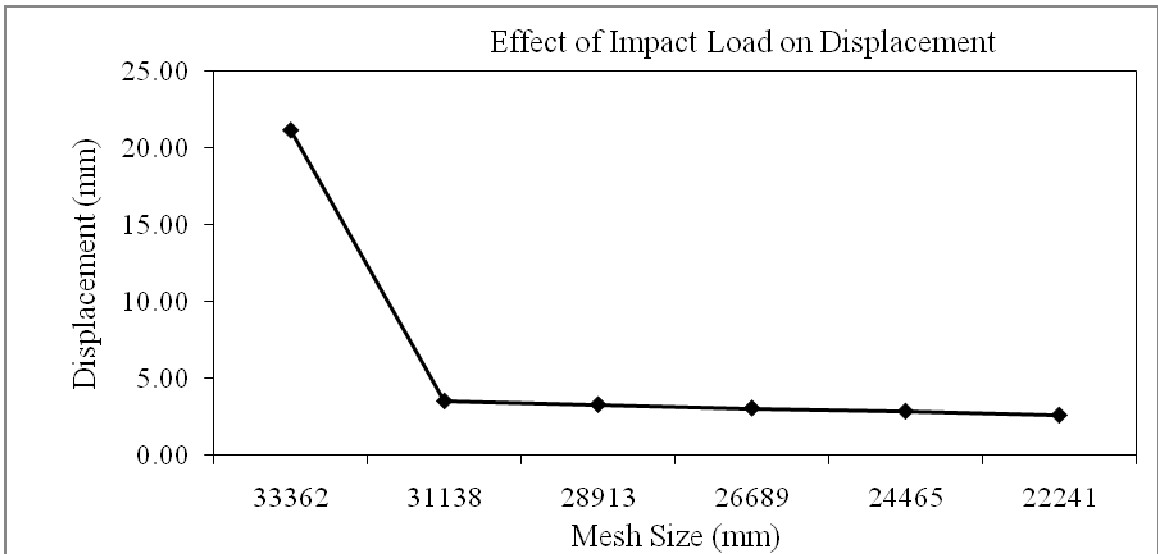


Figure 4.12 Effect of impact load on maximum displacement

It can be concluded from the above results that the frame design is safe for 31,138 N (7000 lbf) static load. Therefore the factor of safety of the existing frame member is 1.2.

#### 4.4 Design modification

Further analysis is carried out to study the influence of other auxiliary plates attached to the frame member as shown in Figure 4.13. These components are welded to the frame to place the engine, transmission and other components of the vehicle. Body sheet panels are also added or welded for the safety and convenience of the drier. The proposed changes for the frame design are:

1. Added/Welded plate at the base of the frame
2. Added/Welded plate to cover the driver sideways and back
3. Added/Welded plate to place the engine and transmission at the back of the frame
4. Added/Welded a pipe at the front bumper of the frame
5. Added/Welded gussets at the front bumper frame members

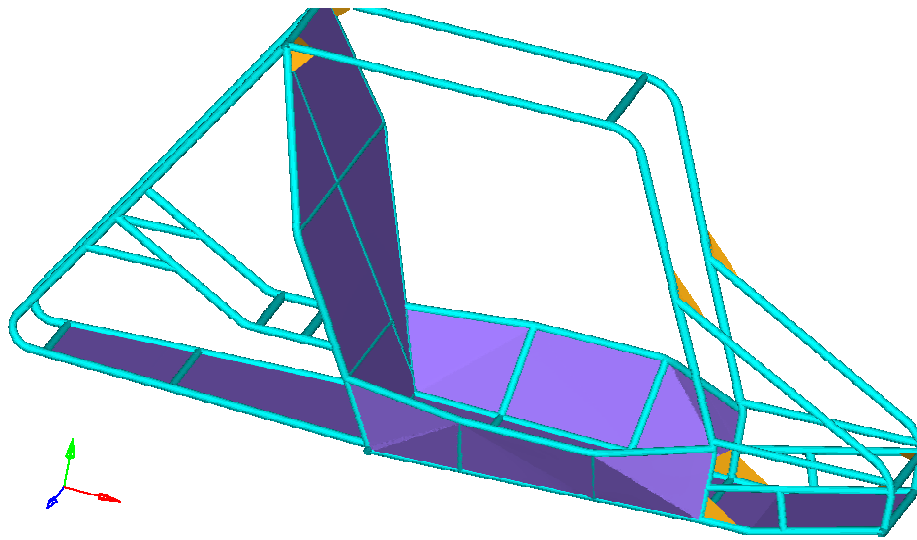


Figure 4.13 New design of the chassis frame/rollcage

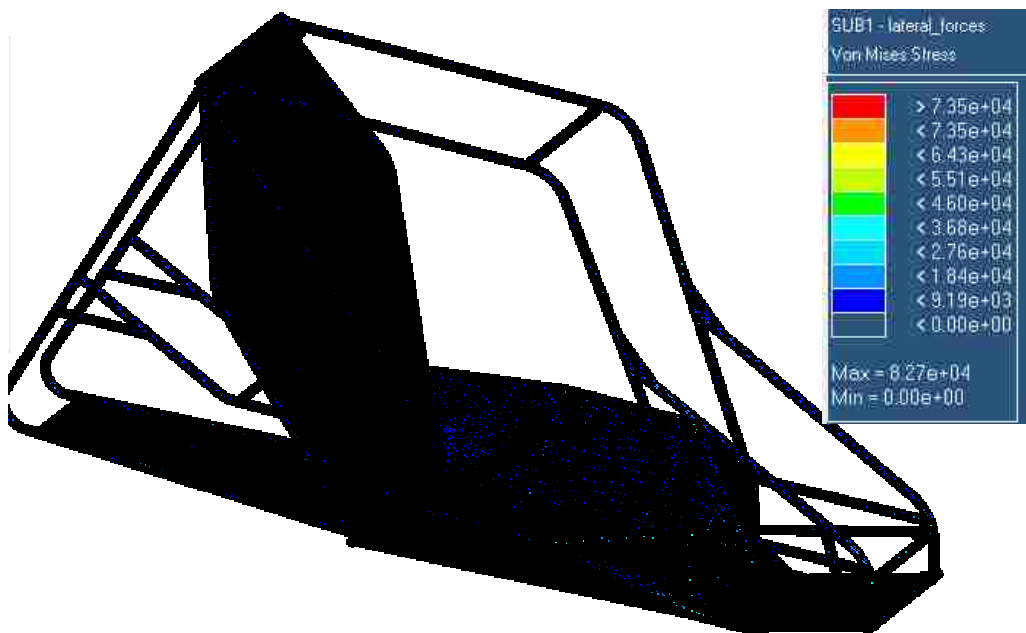


Figure 4.14 Von Mises stress distribution in the frame for 31138 N

impact load

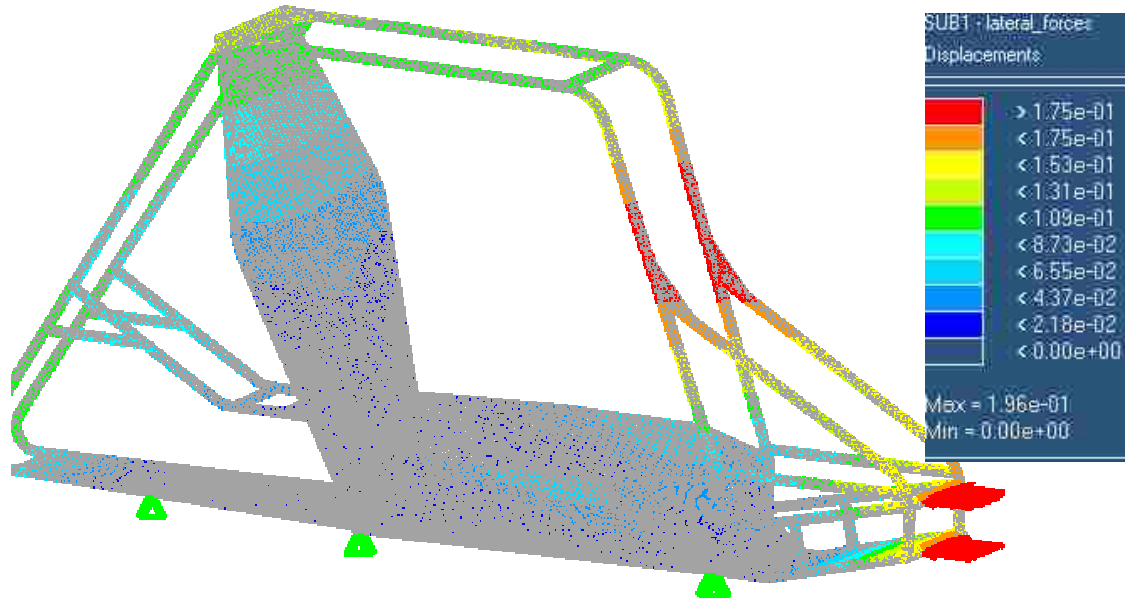


Figure 4.15 Displacement in the frame at 31138 N impact load

The maximum Von Mises stress is 570.2 MPa (82,700 psi), which is less than the yield stress (594.6 MPa) of the frame material. The design is safe for the applied load and is considered for the dynamic crash analysis. The maximum displacement of the frame is 4.98 mm (0.196 in.), which is acceptable for the driver safety.



## CHAPTER 5

### DYNAMIC FRONTAL IMPACT ANALYSIS

#### 5.1 Dynamic Analysis

A multi-body dynamic analysis simulation is carried out to study the performance of the chassis for dynamic loading conditions. This study develops a vehicle chassis model using the multi-body dynamics method to investigate the dynamic response of the chassis/rollcage in a frontal impact. Since the chassis has to provide a base on which various peripherals like engine, power train components, suspension, wheels, steering, driver seating system and other auxiliary components are mounted, modeling was done to distribute the mass of the vehicle over its frame members to simulate the real world problem for dynamic analysis.

The finite element analysis software program used for solving the problem for structural kinematics analysis was LS-DYNA. LS-DYNA is an explicit non-linear dynamic finite element code, which is capable of solving a wide variety of problems including, impact and penetration. In an explicit dynamic analysis, the principle of virtual work is used to write a weak form of an equilibrium equation incorporating the tractions and boundary conditions for each element. This is later summed up over all elements and integrated to obtain the solution for element accelerations. From the explicit solution of elemental acceleration, nodal velocity and

displacements are obtained through integration. Once the displacements are known, incremental strains are computed to update the stress increment through material models and equation of states. In the current research, a frontal impact analysis was run for different loading conditions to study the effect of Von Mises stress, displacement, velocity, acceleration and forces for each loading case. Changes or modifications were done accordingly to the chassis members to withstand the frontal impact crash.

A consistent set of units is specified and used for LS-DYNA modeling. The units used in the FEA models are [18]:

Force: lbf

Length: inches (in.)

Mass: lbf-s<sup>2</sup>/in

Time: sec

A compatibility check for the units used can be conducted by using the definition of force according to Newton's second Law.

By Newton's II law we have,  $F = m * a$

In metric system, the force, mass and acceleration units are lbf, lbf-s<sup>2</sup>/in, and in/s<sup>2</sup> respectively. Therefore  $N = \text{lbf-s}^2/\text{in} * \text{in/s}^2$

$$N = \text{lbf}$$

Therefore the units used are compatible.

## 5.2 Design Methodology for Dynamic Analysis

Following is the generic illustration of the major steps involved in the design process for dynamic analysis. Structurally safe chassis design from linear static analysis is used for accomplishing dynamic analysis.

1. From the existing design, additional geometry members that would be mounted on the chassis like engine, suspension, transmission, driver with seating system and other auxiliary components are modeled as equivalent mass elements for mass distribution of the vehicle to simulate the design for real world dynamic analysis problem.
2. A finite element (FE) model was created using shell elements using Altair HyperMesh, on which dynamic analysis was performed. The element quality has been ensured for optimum FE analysis results.
3. The next step in the analysis was setting the boundary conditions for simulation. The parameters include material properties, section properties, contacts constraints, creating rigid walls, defining initial velocity and other simulation related parameters.
4. After setting the parameters, the simulation was run using LS-DYNA solver for the crash analysis.
5. The results of the simulation were interpreted in HyperView/Ls-Post. The analysis determines the velocity profile, rigid wall forces or reaction forces, total and absorbed energy and acceleration at

any desired location that the frame members are subjected for the applied loading condition.

### 5.3 Geometry Development

For BAJA competition, SAE restricts the teams to use standard engine, power train, steering and other components. The weights of all the components are evaluated and equivalent weights are modeled in the form of solid rigid blocks.

The weight calculations are given below [19, 20]:

Weight of the chassis frame (Includes body sheet & gussets)	- 54.4 kg (120lbs)
Weight of the engine (Briggs & Stratton 10HP)	- 27.2 kg (60lbs)
Weight of tire assembly (Includes suspension 50lbs)	- 45.4 kg (100 lbs)
Weight of transmission	- 27.2 kg (60lbs)
Weight of steering + Brakes & auxiliary components	- 27.2 kg (60lbs)
Weight of the driver	- 90.7 kg (200lbs)
Total weight of the vehicle for simulation	-272.1 kg (600lbs)

In order to reduce the computational time of the simulation, the weights of the above components are defined as lumped mass element assigned to a nodal point or equally distributed to the nodes of a node set different locations using \*ELEMENT\_MASS. Figures 5.1 represent the

equivalent distribution of element masses on the chassis frame for the dynamic analysis.

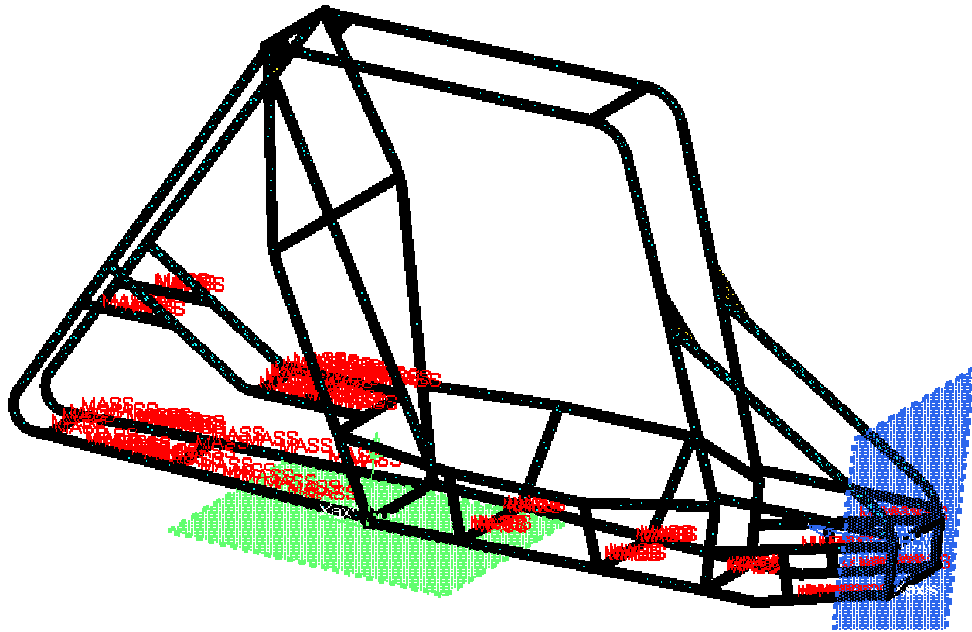


Figure 5.1 Chassis/Rollcage model for multi body dynamic analysis

#### 5.4 Materials

For each component in FEM, a mathematical material needs to be assigned to simulate the behavior of the component. The chassis frame is made of alloy steel 1020 and other components of the vehicle are constructed with different materials. The material behavior and properties of each material is different from others. LS-DYNA has over 100 material models to choose from but due to simplicity of the vehicle model only one of these are selected for the analysis.

#### 5.4.1 \*MAT\_PLASTIC\_KINEMATIC

This material (MAT-3) card was used to model the chassis frame members. This model is suited to model isotropic and kinematic hardening plasticity with the option of including rate effects. It is a very cost efficient material and can be used with beam, shell and solid elements. Table 5.1 represents the material properties for plastic kinematic material model.

Table 5.1 LS-DYNA material models

*MAT_PLASTIC_KINEMATIC					
\$HNAME	MATS	lsteel 1020			
\$#	MID	Rho	E	PR	SIGY
ETAN	BETA				
		17.3300E-0435933000.0		0.3000	86240.0
0.0	0.0				
\$#	SRC	SRP	FS	VP	
	0.0	0.0	0.0	0.0	

#### 5.5 Contact Surfaces

Most of the multi body systems involve contact between different components. In this case contacts are defined between the chassis and

engine, chassis and suspension, chassis and seating (including driver weight) and chassis and bumper members. In actual case all these components are either welded to the frame or fixed through reliable joints to prevent the motion of the components with respect to the chassis. To simulate the equivalent effects in the analysis \*CONTACT\_TIED\_SURFACE\_TO\_SURFACE card is selected for the current problem.

#### 5.5.1 \*CONTACT\_TIED\_SURFACE\_TO\_SURFACE

To ensure proper interaction between components during crash event, contacts between the components have to be specified. LS-DYNA provides an automatic contact formulation between each individual component of the crash model. As currently implemented, one surface of the interface is identified as the master surface and the other as a slave. In tied contact types, the slave nodes are constrained to move with the master surface. At the beginning of the simulation, the nearest master segment for each slave node is located based on an orthogonal projection of the slave node to the master segment. If the slave node is deemed close to the master segment based on established criteria, the slave node is moved to the master surface. In this way, the initial geometry may be slightly altered without invoking any stresses. As the simulation progresses, the iso-parametric position of the slave node with respect to its master segment is held fixed using kinematic constraint equations.

This contact type should generally only be used with solid elements since rotational degrees-of-freedom of the slave node are not constrained.

## 5.6 Rigid Wall

### 5.6.1 \*RIGIDWALL\_PLANAR

RIGIDWALL option provides a simple way of treating contact between a rigid surface and nodal points of a deformable body. \*RIGIDWALL\_PLANAR is LS-DYNA keyword used to define the planar rigid surfaces. It defines a planar wall of finite or infinite size (FINITE). Orthotropic friction can be defined (ORTHO). Also, the plane can possess a mass and an initial velocity (MOVING); otherwise the wall is assumed to be stationary. The FORCES option allows the specification of the segments on the rigid walls on which the contact forces are computed. In order to achieve a more physical reaction related to the force versus tie curve, the SOFT value on the FORCES card can be specified.

## 5.7 Loads and Boundary Conditions

To simulate the chassis crash analysis, all loads and boundary conditions that occur in the actual need to be modeled. Since the current analysis is only limited to chassis crash analysis, the gravitational loads and frictional loads between the tire and road surface are ignored. In the frontal impact or crash testing the vehicle crashes head-on into a rigid concrete barrier at certain speed. A velocity has to be applied to the



vehicle in a manner as to not impart any unrealistic acceleration or cause the simulation to run for an extended amount of time.

### 5.7.1 INITIAL\_VELOCITY\_NODE

This card is used to impart an initial velocity to all the nodes of the vehicle. This card enables a vehicle to start at the prescribed initial velocity without any unrealistic acceleration. It does not require an extended amount of time for the vehicle to ramp up to the prescribed velocity.

The main objective of the frontal impact test is to ensure the chassis frame to be able to dissipate the kinetic energy involved in the crash and the driver is protected from the injurious deceleration forces. The dynamic analysis is carried out for the impact velocity of 15mph. This velocity obviously is lower than typical race track but before a racing car frontally strikes a rigid wall its speed is usually reduced by a gravel run-off areas and the deformable tire barriers. An initial velocity of 15 mph (265 in/s or 6.7 m/s) is ascribed to the whole model to impact a fixed rigid wall.

The energy data can be printed in LS-DYNA file forming a useful check in analysis. The following equation is the energy conservation criteria at all times;

$$E_{kin} + E_{int} + E_{si} + E_{rw} + E_{damp} + E_{hg} = E_{kin} + E_{int} + W_{ext}$$

Where;  $E_{kin}$  = Current kinetic energy

$E_{int}$  = Current internal energy

$E_{si}$  = Current sliding interface energy

$E_{rw}$  = Current rigid wall energy

$E_{damp}$  = Current damping energy

$E_{hg}$  = Current hourglass energy

$E_{kin}$  = Initial kinetic energy

$E_{int}$  = Initial internal energy

$W_{ext}$  = External work

Among those parameters internal energy is the mainly dealt component. In the above equation, Internal energy includes elastic strain energy and work done in permanent deformation. Thus in the model, \*DATABASE\_GLSTAT is activated where the internal energy data is printed.

## 5.8 Frontal Impact Analysis Results Discussion:

Case: Crashworthiness of frame for 15 mph (6.7 m/s) speed of the vehicle against a rigid wall

Figure 5.2 represents the velocity profile of the chassis/rollcage structure for 15 mph (6.7 m/s) impact speed of the vehicle against a rigid wall. The initial velocity of impact is 265 in/s (6.7 m/s). After the impact, the velocity gradually reduces to zero at around 22 ms and becomes negative. The negative velocity is called the rebound velocity. In this case the rebound velocity is 27.1 in/s (2.48 m/s). The total velocity change is 292.1 in/s (26.7 m/s).

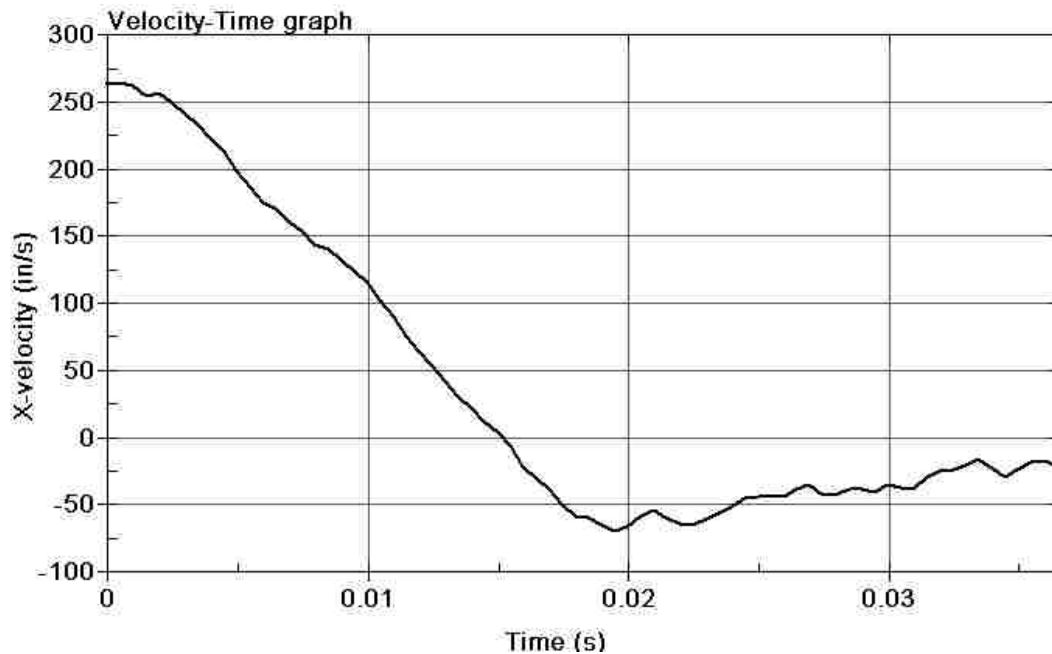


Figure5.2 Velocity profile of the rollcage structure

The rigid wall forces are the reaction force that acts on the frame members during the impact or crash. Figure 5.1 represents rigid wall force history profile of the rollcage structure during the impact. After the impact, the change of momentum from frame structure / rollcage is transferred to the rigid wall that causes high rigid wall forces during initial impact. The maximum rigid wall force is 60,353 lbf (268.5 KN). According to Newton's 3<sup>rd</sup> law, the reaction force on the frame members will also be 60,353 lbf (268.5 KN), which is very high for the cross section of the frame members that cause high deflections in the frame. Figure

5.4 shows the deformation of the frame members at different stages of impact.

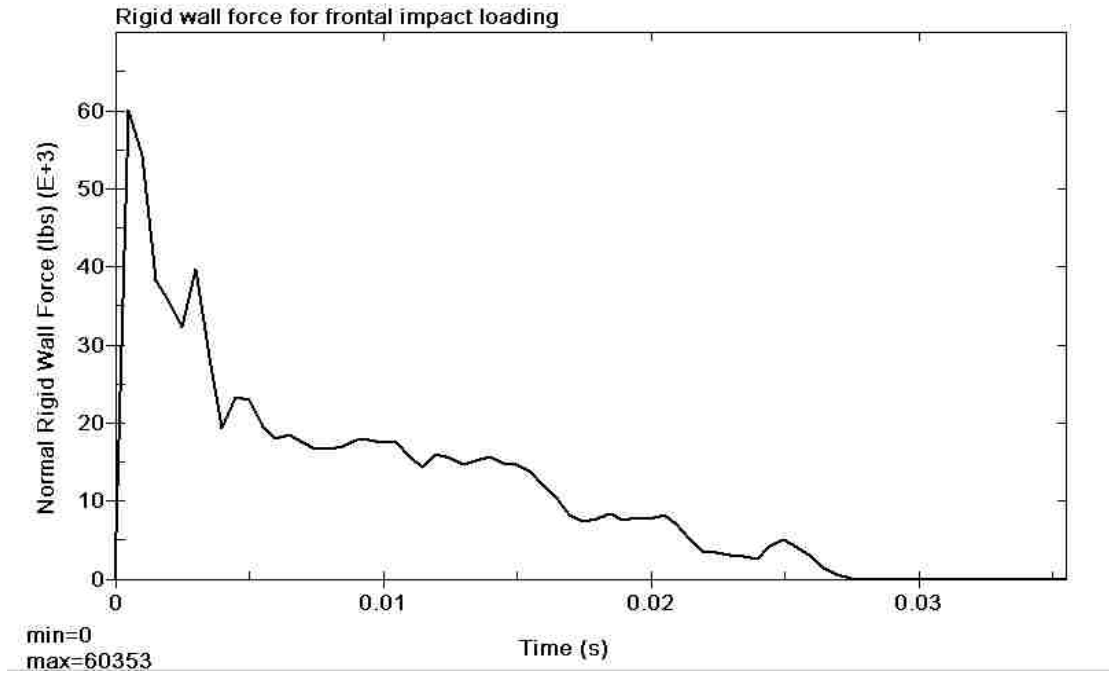
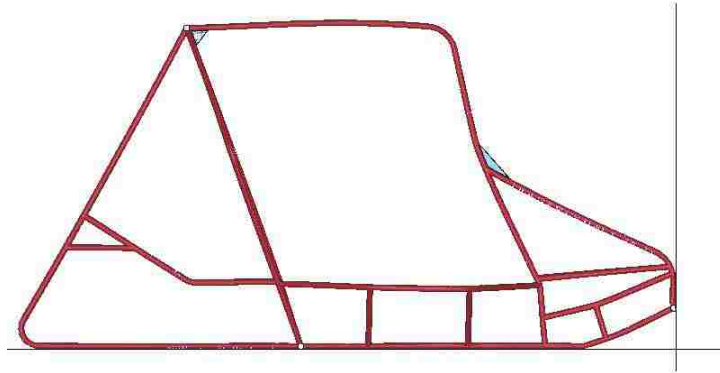


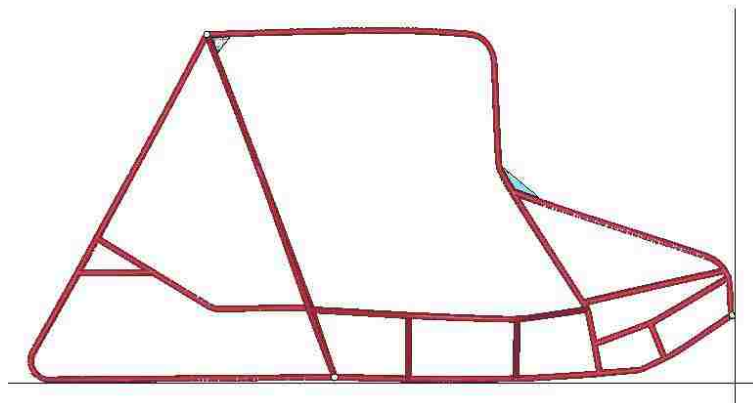
Figure 5.3 Rigid wall force history profile of the rollcage structure during the impact



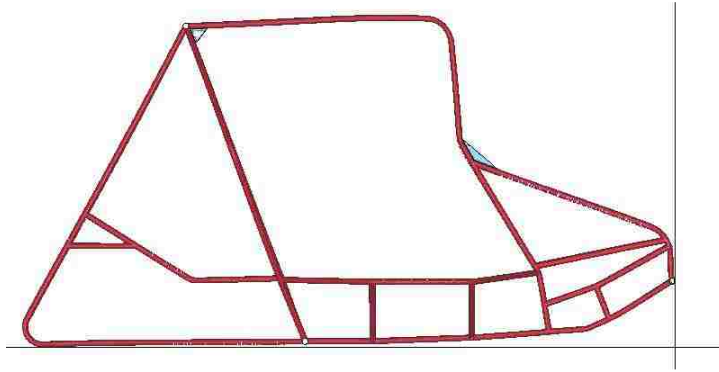
a. Deformation after 5 ms



b. Deformation after 10 ms



c. Deformation after 20 ms



d. Deformation after 30 ms

Figure 5.4 Deformation of the frame members at different stages of impact

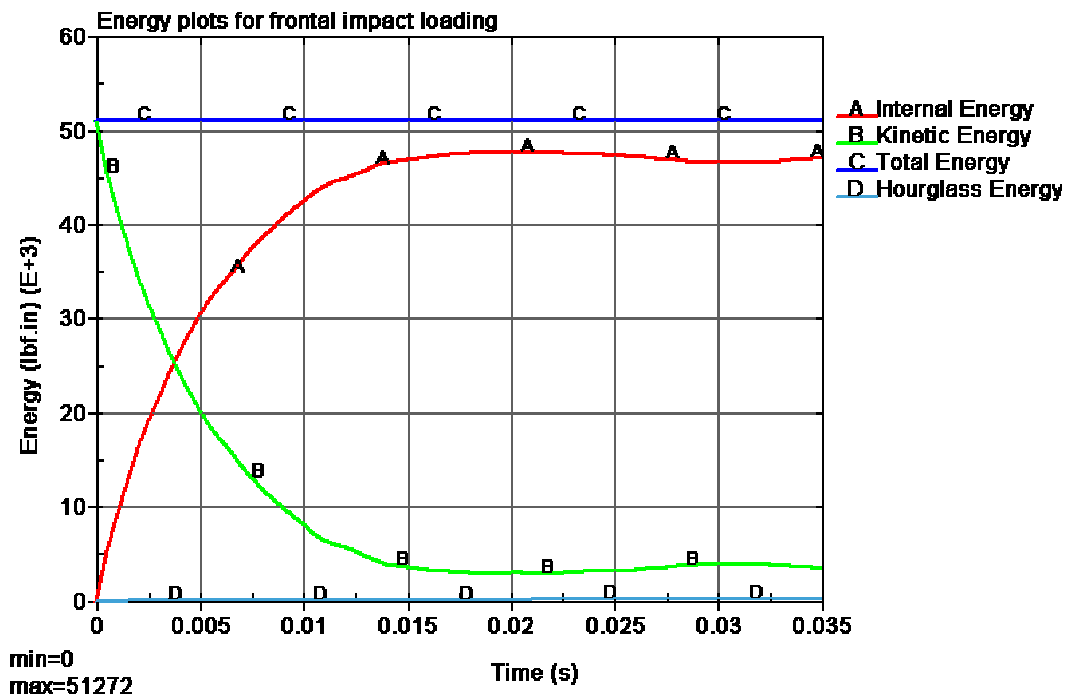


Figure 5.5 Energy plots for impact loading

The energy plot for the frontal crash simulation is shown in Figure 5.5. The total energy is 51,272 in-lbf (5793 J) and is constant throughout the simulation. This shows the conservation of energy is satisfied. It can be observed from the kinetic energy drops drastically when the vehicle hits the rigidwall. The kinetic energy, which is initially at 51,272 in-lbf (5793 J) drops down to about 3000 in-lbf (339 J) and at the same time the internal energy increased to 48,000 in-lbf (5423 J). The hourglass energy is almost zero.

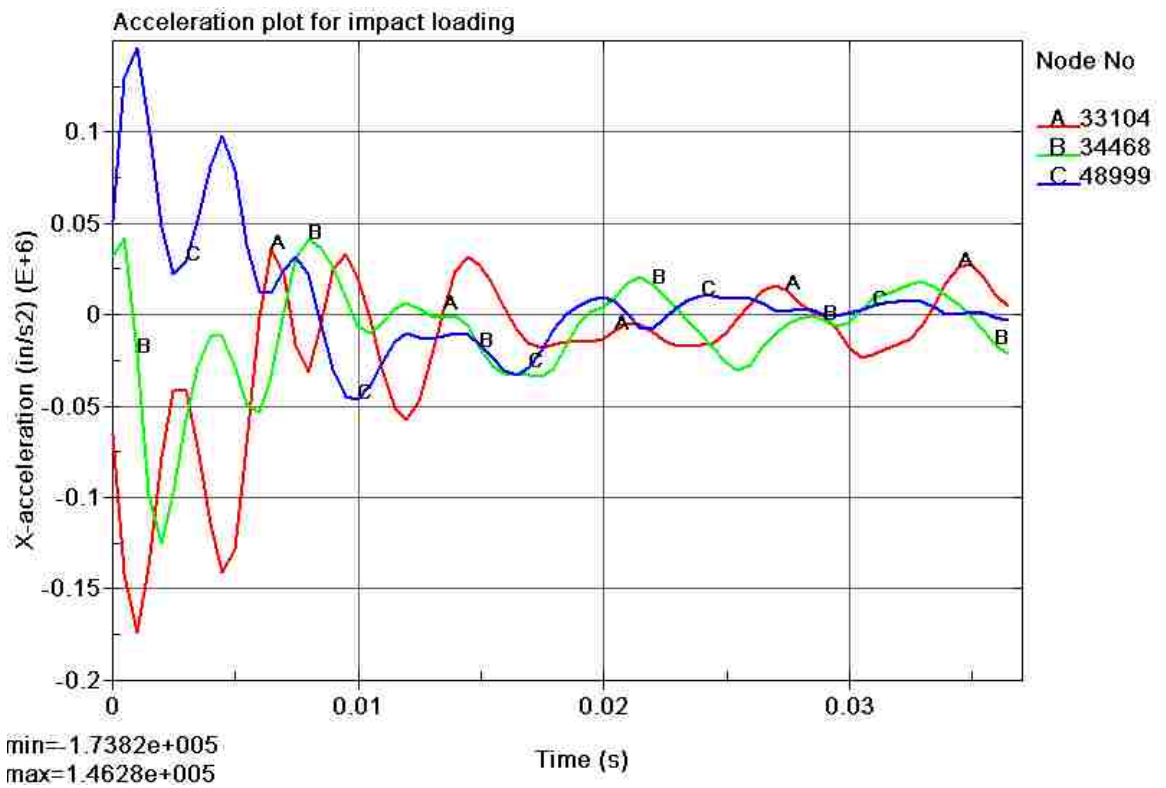


Figure 5.6 Acceleration profiles during the impact

The acceleration is measured at three different nodes at and around the driver location to have an insight of kinematics of the driver during the impact. Figure 5.6 represents the resultant acceleration – time history for the chassis. It is discussed from the result that as soon as the vehicle crash with the rigid wall, the accelerations will reach the peak value of  $0.175e6 \text{ in/s}^2$  ( $4445 \text{ m/s}^2$ ) which is equivalent to 453 G's acceleration. This deceleration is continues for 0.01 s. The decelerations generated in the frame are very that could cause severe head injury and other injuries to the driver.



## CHAPTER 6

### SUMMARY, CONCLUSION AND FUTURE WORK

This chapter provides the summary and outline of the research performed, observations made from the different structural analysis on a rollcage frame for SAE BAJA competition. Finally, recommendations for future work that would build on this research were discussed.

#### 6.1 Research Summary and Conclusion

The usage of finite element analysis was invaluable to the design and analysis of the frame for SAE Baja Vehicle. The objective of the present research is to perform finite element structural analysis on rollcage frame and optimize the design for different loading conditions. Structural analysis in the research includes the linear static and dynamic analysis for simulating the impact loading. The static analysis was aimed to determine the optimum mesh size and to study the effects of stress and displacement on the rollcage frame members. Yielding is considered to be the failure criteria for the static analysis.

A preliminary design of the rollcage was produced based on the rules of the competition using CAD. This CAD design model was used to perform the FE analysis. A finite element simulation for frontal impact load of 33,362 N (7500 lbf) was carried out for a design factor of safety of 1.25 on the rollcage frame to investigate the effects of stress and strain for the applied load. The design has got convergence for a grid size of

4.24 mm. The max displacement of the frame was 25.1 mm and max Von Mises stress generated for the grid size was 958.37 MPa which is higher than the yield stress of the material of the frame (594.6 MPa).

Based on the stress pattern in the frame, gussets were provided at the maximum stress locations to reduce the stress concentration by distributing the force of impact further down the intersecting members. Frontal impact analysis was carried out to optimize the size of the gussets. It was been concluded that the optimum gusset size for the design of the frame was 88.9 mm L X 88.9 mm H X 6.35 mm T (3.5 in. L x 3.5 in. H x 0.25 in. T). The displacement of the members was favorable enough for the safety of the driver. The maximum stress was reduced by 21.87 % with the gussets. But this stress 751.53 MPa was also higher than the yield stress and design was not safe for a factor of safety 1.25.

An attempt was done to find out the safe load for the design of the frame. The OptiStruct simulation was carried out on the gusset frame design for different impact loads varied from 33,362 N (7500 lbf) to 22,241 N (5000 lbf). It can be concluded from the above results that the frame design is structurally safe for a load below 31,138 N (7000 lbf) static. Therefore the factor of safety of the existing frame member is 1.2.

Another objective of the present research was to accomplish the dynamic analysis on the structurally safe rollcage frame to review the structural rigidity and the injury criteria. A full vehicle modeling was

carried out for the equivalent mass distribution of the vehicle. An initial velocity of 15 mph (265 in/s) is ascribed to the full vehicle model to impact a fixed rigid wall to investigate the effects of dynamic stresses, energy, forces and acceleration of the frame members.

Dynamic frontal crash analysis on rollcage structure revealed high level of reaction forces (60,353 lbf) and acceleration (453 G's) during the impact. The total energy after the impact is directly transferred by the frame members that create severe deformations in the frame. A further research has to be carried to reduce the generated accelerations on the frame members.

The current research provides a standard finite element analysis procedure for designing future SAE Baja vehicle chassis/rollcage. It can be concluded from this research that the future SAE BAJA teams should use the static analysis to evaluate the stresses and deformations in the frame before building the rollcage structure. A multi body dynamic crash analysis is an option for the SAE BAJA team to understand the exact behavior of the frame for frontal impact, to study the effects of forces and acceleration during the impact. Modifications to the existing frame members should be done at every stage of the analysis depending on the simulation results for the safe design. This report includes the criterion for the safe design for static and dynamic frontal impact analysis. The engineers to build the rollcage structure use the safe design. Following

the standard procedure would help the engineers to reduce the weight of the rollcage without affecting the structural strength thus improves the vehicle performance and driver safety.

## 6.2 Future Work

- Present research only focused on the frontal impact analysis of the rollcage structure. There are other loading conditions to be analyzed to evaluate the accurate structural behavior of the frame members. The other loading conditions include rollover loading (static and dynamic), side impact loading, heave loading and shock mount loading etc.
- In addition to the rollcage optimization, there is a scope for further research on optimization of the drive train, suspension, brakes and wheels to enhance the performance of the Baja vehicle.
- Current research considers only one material option for the roll-cage. Further research should explore the effect of material modeling to reduce the weight of the roll-cage.
- The present research on the frontal impact analysis focused on one frame material type and bumper material type to reduce the accelerations. Further research has to be carried out towards material modeling has to be done to reduce the generated accelerations and reaction forces on the rollcage structure and to find out the optimum material properties for the rollcage structure.

## REFERENCES

1. 2009 Baja SAE Competition Rules  
[\(<http://www.sae.org/students/mbrules.pdf>\)](http://www.sae.org/students/mbrules.pdf).
2. University of Tennessee at Chattanooga, "Mini Baja Design Report 2006".
3. Union College SAE Baja Vehicle Design Report 2005.
4. Mark, Wan. "Different Types of Chassis." Autozine. 2000. Autozine Technical School. 21 Mar. 2006,  
[http://www.autozine.org/technical\\_school/chassis/tech\\_chassis.htm](http://www.autozine.org/technical_school/chassis/tech_chassis.htm)
5. Abhijit Duraphe, Ajit D. Kelkar and David Klett, "Non-Linear Structural Analysis of an All Terrain Vehicle Using Ansys",  
<http://www.ncat.edu/~duraphe/pub/Ansys.pdf>.
6. University of Nevada Las Vegas, "Baja SAE Technical Design Report 2008".
7. Mark Anthony Virginia, "Crashworthiness of a pre NCAP safety standard light truck and corresponding suspension analysis" A thesis Report, Wichita state University 2001.
8. Side Impact Crashworthiness Evaluation, Crash Test Protocol (Version V), IIHS, May 2008  
[\(\[http://www.iihs.org/ratings/protocols/pdf/test\\\_protocol\\\_side.pdf\]\(http://www.iihs.org/ratings/protocols/pdf/test\_protocol\_side.pdf\)\)](http://www.iihs.org/ratings/protocols/pdf/test_protocol_side.pdf).
9. Altair Hyperworks 10.0 User Manual.

10. "LS-DYNA theoretical manual," Livemore Software Technology Corporation.
11. Sane, S.S., Ghanashyam Jadav, and Anandraj, H., "Stress analysis of a light commercial vehicle chassis by FEM", p1-5, Driving Innovation with enterprise simulation.
12. Worcester Polytechnic Institute, "SAE Baja Design Report 2006".
13. Jonathan Hastie, Mini Baja Vehicle Design Optimization, Honors Thesis, Fall 2004 – Fall 2005.
14. Anthony Taylor Owens, Marc Daniel Jarmulowicz, Peter Jones, "Structural Considerations of a Baja SAE Frame", Motorsports Engineering Conference & Exposition, December 2006.
15. Florida Institute of Technology, " Mini Baja design Report 2008".
16. Vijay Jain, Manvinder Singh, "Mini Baja Design Report",  
<http://www.freewebs.com/manvinder/baja.pdf>
17. 2008-2009 Design and Fabrication of a SAE Baja Race Vehicle, A Major Qualifying Project Report, Worcester Polytechnic Institute.
18. LS-DYNA Support,  
<http://www.dynasupport.com/howtos/general/consistent-units>
19. Briggs and Stratton website. <[www.briggsracing.com](http://www.briggsracing.com)>
20. The Buggy Shop <[thebuggyshop.50megs.com](http://thebuggyshop.50megs.com)>
21. "LS-DYNA version 970 keyword user's manual," Livermore Software Technology Corporation.

22. Mehrdad Asadi, Brian Walker, Hassan Shirvani, “New Finite Element Model for NHTSA Impact Barrier”, 10th International LS-DYNA® Users Conference.
23. CYMAT Material Data Sheet,  
<http://www.alusion.com/download/Cymat%20Technical%20Manual%20Nov%202009.pdf>
24. [www.matweb.com](http://www.matweb.com)

## APPENDIX A

### SAE BAJA RULES 2009

#### SECTION 3: ROLL CAGE, SYSTEMS & DRIVER'S EQUIPMENT

##### 30. INTRODUCTION

The following design requirements apply to all Baja competitions. The design and technical rules will be strictly enforced. It is the responsibility of each team to meet all technical requirements using sound engineering principles and construction done meeting proper fabrication procedures. Failure to do so may mean disqualification from the competition; final judgment rests with the National Technical Inspectors. If you have any doubts about any technical requirement, please pose questions by email to [basrules@sae.org](mailto:basrules@sae.org). National Technical Inspectors will do their best to answer these questions within two weeks. Please include your name, school, contact information and the rule number in question in your email.

##### 30.1 Rules Requirements and Restrictions

###### 30.1.1 Technical Inspection

All Baja vehicles must pass a technical inspection before they are permitted to compete. Once a vehicle has passed technical inspection, it must remain "as approved" condition throughout the competition. Repairs must be made with parts that are identical. Parts that are not identical, must get approved from a National Technical Inspector prior to replacement.

###### 30.1.2 Required Modifications

All installation and construction are subject to the approval of the technical inspectors, who may require modifications at their discretion. All competitors should be prepared to note these modifications during technical inspections.

###### 30.1.3 Unstable Vehicles

Any vehicle exhibiting handling or other vehicle dynamics that are deemed unstable by the technical inspectors will not be permitted to participate in the dynamic events.

##### 31. ROLL CAGE

###### 31.1 Objective

The purpose of the roll cage is to provide a minimal three-dimensional space surrounding the driver. The cage must be designed and fabricated to prevent any failure of the cage's integrity. The cage must be large enough for:

1. The driver's helmet to be 15.24 cm (6 in) away from the straightedge applied to any two points on the cockpit of the car, excluding the driver's seat and the rear driver safety supports.
2. The driver's torso, knees, shoulders, elbows, hands, and arms must have a minimum of 7.62 cm (3 in) of clearance from the envelope created by the structure of the car. (This is tested by applying a straight-edge between any two points on the outside edges of the SEM and RHO, less the roll cage padding.)

###### 31.2 Roll Cage Requirements

###### 31.2.1 Elements of the Roll Cage

The elements of the roll cage that must meet the material specification per 31.5:

- Rear Roll Hoop (RRH) Rule 31.2.2
- Roll Hoop-Overhead Members (RHO) Rule 31.2.4
- Front Bracing Members (FBM) Rule 31.2.7
- Lateral Cross Member (LC) Rules 31.2.4 and 31.2.5



Additional required members must be steel and only have a maximum thickness of .89 mm (.035 in) and a minimum outside diameter of 2.54 cm (1.0 in) and are as follows:

- Lateral Diagonal Bracing (LDB)
- Lower Frame Side (LFS)
- Side Impact Member (SIM)
- Fore/Aft Bracing (FAB)
- Front Lateral Cross Member (FLC)
- Under Seat Member (USM)

Any tube that is used to mount the safety belts  
 Reference points: See drawings in this section.

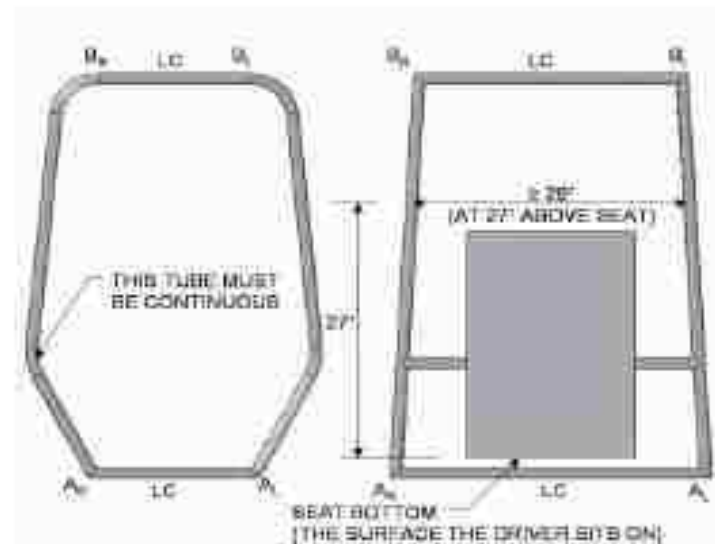
**NOTE:** When minimal dimensions are given that is to the centerline of the members, and when a clearance for the driver is given, it is defined by the outside edges of the roll cage members less the padding installed.

\*All roll cage members having a bend radius  $\geq 15.2$  cm (6 in) may NOT be longer than 71.1 cm (28 in) unsupported.

**Definition – DRIVER** – For the purpose of this section “driver” refers to the team’s largest driver and the 95<sup>th</sup> percentile male properly suited and wearing a helmet.

31.2.2 Rear Roll Hoop (RRH)

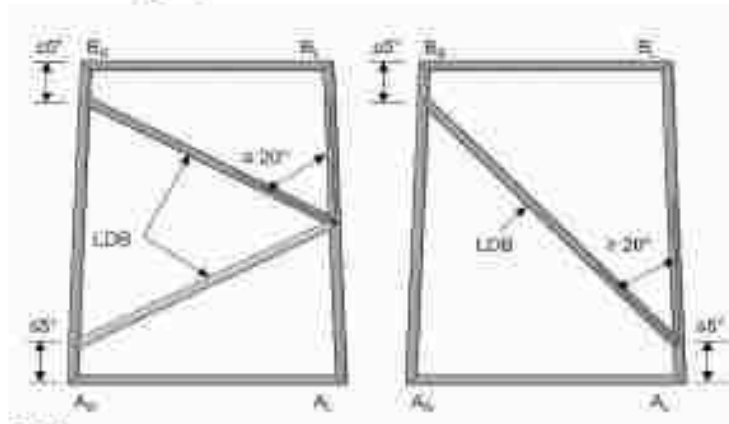
The RRH is made up of a maximum of four sections: two LC at highest and lowest points and two continuous, no break vertical members. This may be one continuous hoop/tube. The driver’s seat may not intrude into the plane(s) of the RRH. The upper junctions in straight tube construction shall define points B<sub>H</sub> and B<sub>L</sub>. If bend-tube construction is used, points B<sub>H</sub> and B<sub>L</sub> will occur at the upper end of each bend (See RC1). The RRH shall extend upward vertically  $\sim 20$  degrees from points A to points B. The RRH must also be a minimum of 73.6 cm (29 in) wide at 68.6 cm (27 in) above the driver’s seat (checked by a template).



31.2.3 Rear Roll Hoop Lateral Diagonal Bracing (LDB)

Lateral bracing for the Rear Roll Hoop will begin at a point along the vertical portion of the RRH where the edge of the joint is within 12.7 cm (5 in) vertically of point B<sub>0</sub> or B<sub>1</sub> and extend diagonally to an edge of a joint no farther than 12.7 cm (5 in) above point A<sub>R</sub> or A<sub>L</sub> (See RC2). The vertical angle between the RRH and the LDB must be no less than 20 degrees.

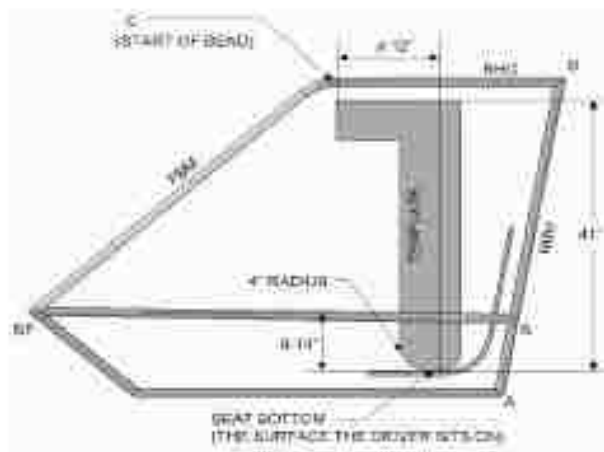
Lateral bracing may consist of two or more members.



RC 2

31.2.4 Roll Hoop Overhead Members (RHO)

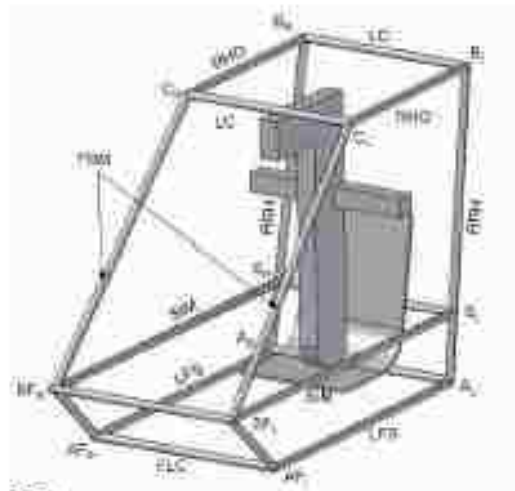
Roll Hoop Overhead members shall join the RRH within 5.1 cm (2 inches) vertically or laterally of points B and extend generally horizontal to point C. The tubes must be continuous and no break members from point B to point C are allowed. The RHO shall be located above the driver's seat by a minimum of 104.1 cm (41 inches). Points C should be located forward of the driver's seat by a minimum of 30.5 cm (12 inches). (See RC3). Points C<sub>0</sub> and C<sub>1</sub> shall be joined by a lateral cross member (LC).



RC 3

**31.2.4.1 Lower Frame Side Members (LFS)**

Lower frame side members shall join the RRH and LC and extend to points forward of the driver's heel to a front internal cross member (FLC) (See RC4).



**RC 4**

**31.2.5 Side Impact Members (SIM)**

Side impact members shall join the RRH at points S and extend horizontally to points SF forward of the driver's toes (See RC4). The SIM shall be between 20.3 cm (8 inches) and 35.6 cm (14 inches) (as measured vertically) above the area of the seat in contact with the driver (See RC3).

**NOTE:** The driver's feet must be behind the plane created by points AF<sub>1,1</sub> and SF<sub>1,1</sub>. If the tube between SF<sub>1,1</sub> is below the driver's toes then an additional bar will be required above the driver's toes (The intent of this is to protect the driver's feet from a tire intrusion).

**31.2.6 Under Seat Member (USM)**

An under seat member (USM) shall attach to the LFS members, and pass beneath the seat. The USM shall be positioned in such a way to prevent the seat and/or driver from passing through the plane of the LFS in the event of seat failure.

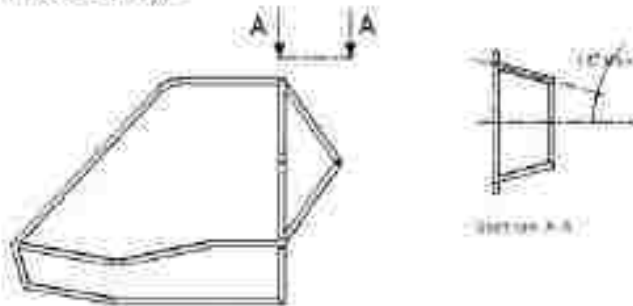


**31.2.8.1 Front Bracing**

If front bracing is used it must connect FBM<sub>UP</sub>, LFS and the SIM. Front bracing must be attached as close as possible to the top of the roll cage (Point C).

**31.2.8.2 Rear Bracing**

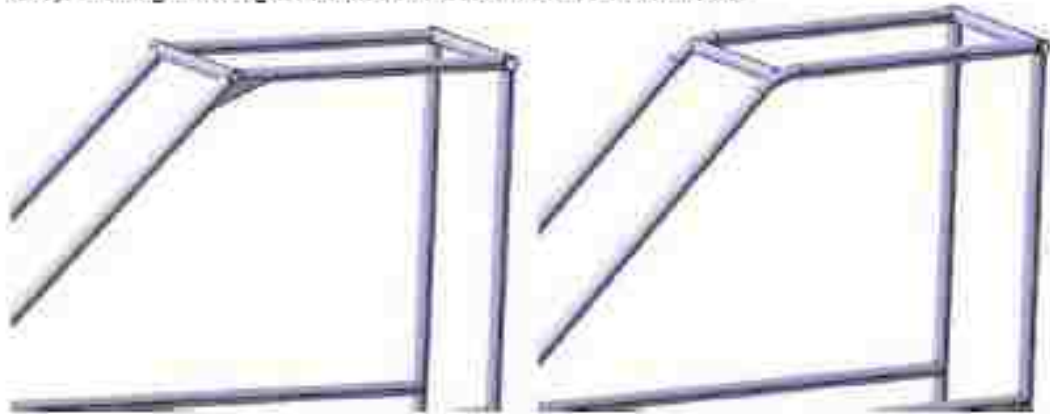
If rear bracing is used it must be attached as close as possible to the top of the roll hoop along the outer perimeter. The bracing must be triangulated and connect back to the RRH at or below the SIM. From a top view, plane created by the RHB members shall be maximum of 15 degrees from the plane created by the RRH (see figure 31.2.8.2.1). The RHB members on the right and left side shall be connected by a cross member at the node or as close as possible to the bend which makes up the vertex of the RHB.



**RC 7**

**31.2.9 RHO/FBM Gusseting**

If the RHO and FBM are not fabricated from a continuous tube, a gusset is required at point C. Gussets shall be made of steel by two methods. 1.) Steel tubing meeting the min requirement of 31.2.1 or 2.) Steel plate, be triangular from a side view, and have a minimum thickness of 0.065". The gussets shall be welded to the sides of the tubes and not directly in the plane of the tubes making up each joint (See RC6). The length of the gusset must be at least 3 times the tube diameter.

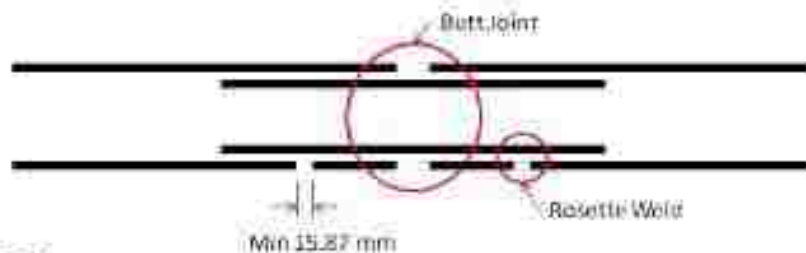


**RC 8**

The example on the left shows a design where gusseting is required at point C, the example on the right shows a frame where gusseting would not be required at point C.

31.2.10 Butt Joints

All butt joints within any of the elements on the roll cage listed in section 31.2.1 (excluding the required no break members described in 31.2.2, 31.2.4 and 31.2.7) must be reinforced with a welded sleeve. A butt joint is defined as a joint where two tubes come together generally along the same line and are not supported by a third tube at the node. The sleeve must be designed to tightly fit on the inside on the joint being reinforced (i.e. external sleeves are not allowed), must extend into each side of the sleeved joint, a length of at least two times the diameter of the tubes being reinforced, and be made from steel at least as thick as the tubes being reinforced. In addition to meeting basic geometry requirements, the sleeve must be designed and fabricated to both reinforce the joint and to distribute the stress concentrations of the best affected zone. A minimum of 4 linear inches of weld length is required to secure the sleeve inside the joint, and the welds must be clearly visible from the outside of the joint. Refer to Figure # below.



RC 9

31.2.11 Weld Confirmation Checks

Teams must conduct weld confirmation testing for each welder that welds their vehicle roll cage. The team must demonstrate its ability to produce welded joints of a known quality with materials, tools and procedures similar to those being used in the fabrication of the chassis. The team must conduct destructive testing using the following requirements.

The following definitions will apply to the entirety of rule 31.2.11:

- As-Built Vehicle: the vehicle presented at technical inspection
- Roll Cage Elements: elements of the roll cage as discussed in rule 31.2.1
- Roll Cage Welds: any weld joining two or more roll cage elements or one or more roll cage elements and one or more gussets as discussed in rule 31.2.9
- Roll Cage Material: tubing of the same geometry and alloy as the roll cage elements of the as-built vehicle
- Roll Cage Welder: any person that performs welding of the roll cage welds of the as-built vehicle

Each roll cage welder must demonstrate sufficient welding skill and craftsmanship with the tools, processes and roll cage material. In addition to visual inspection of the as-built vehicle, the national technical inspectors will collect and inspect welding samples during the technical inspection process to determine dynamic and endurance event competition eligibility. Teams unable to submit welding samples of adequate quality, as defined below, shall not be eligible to compete in any dynamic or endurance event.

Each team must submit two (2) samples for each roll cage welder, both of which are constructed of roll cage material which have been welded with the same tools and processes as those of the as-built vehicle and which have also been subject to the following destructive testing and inspection:

**Sample 1 – Destructive Testing**

A structure made up of roll cage tubing welded at a 90 degree angle, the length of each tube to be determined by the team. < Figure 3 > This joint should be subject to destructive testing causing the joint to fail to which indicates superior weld strength with respect to the base material. (The testing method is left to the team's discretion. For example, teams can do pull testing in a lab, or apply a moment to one side of the joint while fixing the other side of the joint.)

Figure 3

**Sample 2 – Destructive Inspection**

A structure made up of roll cage material that has two tubes attached at a 30 degree angle with a length of at least 15cm from the center of the weld joint. < Figure 4 > The sample should be sectioned along the length of tube to reveal adequate and uniform weld penetration < Figure 5 >



Figure 4



Figure 5

Final judgment of weld strength with respect to the base material as it described in sample 1 and the adequacy and uniformity of weld penetration as described in sample 2 shall rest with the national technical inspectors. Sample documents of OK welds and NG welds will be provided on the SAE website.

Welding samples constructed of material other than the roll cage material and / or welded with a process other than that of the roll cage welds of the as-built vehicle shall not be considered sufficient demonstration of welding skill and craftsmanship with the tools, processes and roll cage material.

Note: Frames that were constructed in a previous year will need to have samples welded by that welder or remove two sections of the current frame and perform the tests on these components.

### 31.2.12 Final Judgment

The rules are considered a minimum, but the final judgment will rest with the National Technical Inspectors. If during the event, any frame shows signs of yield and/or failure the car will be removed from competition until the technical inspectors confirm that the frame complies with the rules again.

**Comment:** In all cases, especially bent tube construction, technical inspectors may require additional bracing if they feel the roll cage does not offer adequate protection. Any tubes showing cracks and deformation do not comply with the rules.

### 31.3 Head Restraint

A head restraint must be provided on the car to limit rearward motion of the head in case of an accident. The restraint must have a minimum area of 232 sq. cm (36 sq inches), and be padded with a foam that meets SFI 45.2 specifications. The Foam cannot have more than 3 layers laminated together to create the 5.08cm thickness. The restraint must be a minimum thickness of 5.08cm (2.0 inches), and be located no more than 2.5 cm (1 inch) away from the helmet in the uncompressed state. The head restraint must be mechanically fastened (NO Velcro or adhesive) to the vehicle, preferably the vehicle frame. Head restraints may also be mechanically fastened or integral to the driver's seat. The head restraint must meet the above requirements for all drivers. For a listing of manufacturers of SFI 45.2 foam, see: <http://www.sfi.com/faq.htm#sfi45.2>

### 31.4 Driver Head Clearance

For driver head clearance, the roll cage must extend a minimum of 104.1 cm (41 inches) above the seating surface to the bottom of the upper roll cage tubes measured vertically using the template in RC 3. The template radiused bottom should be placed in the joint of the seat base and the seat backrest and positioned vertically. The template "tee" top describes the projection of the required clearance height forward and rearward. While the template fixes the clearance height forward, the clearance height rearward must be extended in each design over the helmet top of a seated and secured driver. Taller drivers may be accommodated by lengthening the template vertical member and raising the entire clearance height envelope above the 104.1 cm (41 inches) minimum.

#### 31.4.1 Head Clearance – Minimum

In all cases, a minimum of 15.2 cm (6 inches) vertical clearance must be provided from the helmet top of the team's tallest driver to the bottom of the roll cage top tubes or members.

### 31.5 Roll Cage & Bracing Materials

The material used for the entire required roll cage members specified in 31.2.1 must, at minimum, be:

(A) Circular steel tubing with an outside diameter of 25mm (1 inch) and a wall thickness of 3 mm (.120 inch) and a carbon content of at least 0.18%

OR

(B) If the standard tubing sized specified above are not used, required roll cage members must be made of steel with at least equal bending stiffness and bending strength to 1018 steel having a circular cross section with a 25.4 mm outer diameter and a wall thickness of 3.05 mm, nominally. All calculations showing the equivalence must be in SI units. Calculations proving equivalence must be performed using three significant figures to the nominal tube sizes as specified by the vendor on the invoice.

**NOTE:** The use of alloy steel does not allow the wall thickness to be thinner than 1.57 mm (.062 inch).



**31.2.12 Final Judgment**

The rules are considered a minimum, but the final judgment will rest with the National Technical Inspectors. If during the event, any frame shows signs of yield and/or failure the car will be removed from competition until the technical inspectors confirm that the frame complies with the rules again.

**Comment:** In all cases, especially bent tube construction, technical inspectors may require additional bracing if they feel the roll cage does not offer adequate protection. Any tubes showing cracks and deformation do not comply with the rules.

**31.3 Head Restraint**

A head restraint must be provided on the car to limit rearward motion of the head in case of an accident. The restraint must have a minimum area of 232 sq. cm (36 sq. inches), and be padded with a foam that meets SFI 45.2 specifications. The Foam cannot have more than 3 layers laminated together to create the 5.08cm thickness. The restraint must be a minimum thickness of 5.08cm (2.0 inches), and be located no more than 3.5 cm (1 inch) away from the helmet in the uncompressed state. The head restraint must be mechanically fastened (NO Velcro or adhesive) to the vehicle, preferably the vehicle frame. Head restraints may also be mechanically fastened or integral to the driver's seat. The head restraint must meet the above requirements for all drivers. For a listing of manufacturers of SFI 45.2 foam, see: <http://www.affoundation.com/manuf.html#45.2>

**31.4 Driver Head Clearance**

For driver head clearance, the roll cage must extend a minimum of 104.1 cm (41 inches) above the seating surface to the bottom of the upper roll cage tubes measured vertically using the template in RC 3. The template radiused bottom should be placed in the joint of the seat base and the seat backrest and positioned vertically. The template "tee" top describes the projection of the required clearance height forward and rearward. While the template fixes the clearance height forward, the clearance height rearward must be extended in each design over the helmet top of a seated and secured driver. Taller drivers may be accommodated by lengthening the template vertical member and raising the entire clearance height envelope above the 104.1 cm (41 inches) minimum.

**31.4.1 Head Clearance – Minimum**

In all cases, a minimum of 15.2 cm (6 inches) vertical clearance must be provided from the helmet top of the team's tallest driver to the bottom of the roll cage top tubes or members.

**31.5 Roll Cage & Bracing Materials**

The material used for the entire required roll cage members specified in 31.2.1 must, at minimum, be:

(A) Circular steel tubing with an outside diameter of 25mm (1 inch) and a wall thickness of 3 mm (.120 inch) and a carbon content of at least 0.28%.

OR

(B) If the standard tubing sized specified above are not used, required roll cage members must be made of steel with at least equal bending stiffness and bending strength to 1018 steel having a circular cross section with a 25.4 mm outer diameter and a wall thickness of 3.05 mm, nominally. All calculations showing the equivalence must be in SI units. Calculations proving equivalence must be performed using three significant figures to the nominal tube sizes as specified by the vendor on the invoice.

**NOTE:** The use of alloy steel does not allow the wall thickness to be thinner than 1.57 mm (.062 inch).

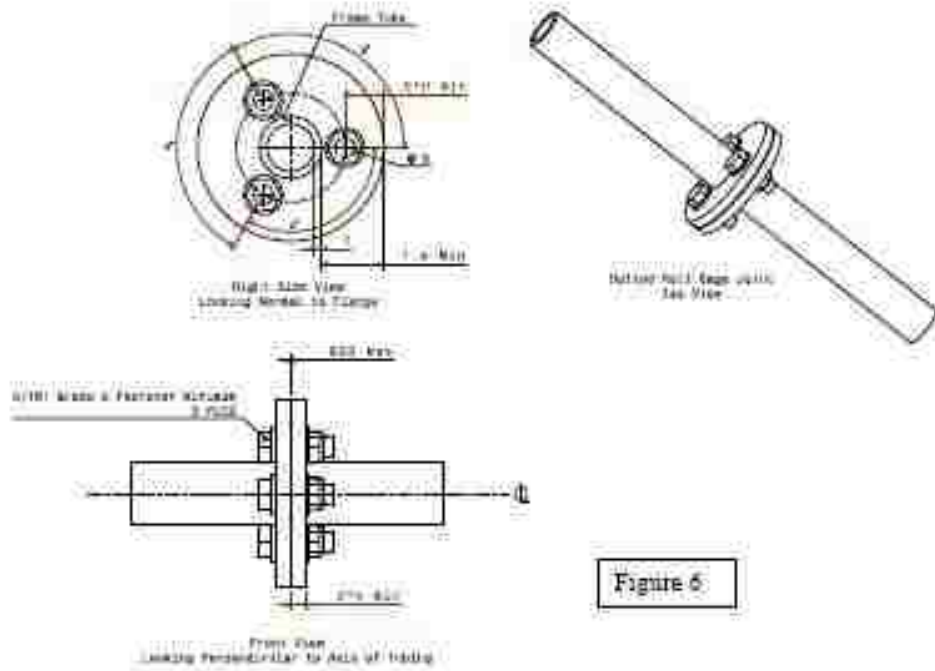


Figure 6

31.8.1 Unacceptable Bolted Roll Cage Joint



32. COCKPIT

32.1 Design Objective

The cockpit must be designed to (1) protect the driver and (2) permit easy driver exit in an emergency.

## APPENDIX B

### EXAMPLE LS-DYNA PROGRAM

```

$$ HM_OUTPUT_DECK created 16:36:19 05-18-2010 by HyperMesh Version
9.0b121
$$ LS-DYNA Input Deck Generated by HyperMesh Version : 9.0b121
$$ Generated using HyperMesh-LS-DYNA 971 Template Version : 9.0b121
*KEYWORD
*CONTROL_TERMINATION
$$  ENDTIM      ENDCYC      DTMIN      ENDENG      ENDMAS
      0.05
*CONTROL_TIMESTEP
$$  DTINIT      TSSFAC      ISDO      TSLIMIT      DT2MS      LCTM      ERODE
MSIST
      0.0      0.9
*CONTROL_HOURLASS
$$   IHQ      QH
      1      0.1
*CONTROL_ENERGY
$$   HGEN      RWEN      SLNTEN      RYLEN
      2      2      2
$$DATABASE_OPTION -- Control Cards for ASCII output
*DATABASE_ELOUT
1.0000E-03      1
*DATABASE_GLSTAT
1.0000E-03      1
*DATABASE_MATSUM
1.0000E-03      1
*DATABASE_NODOUT
1.0000E-03      1
*DATABASE_RWFORC
1.0000E-03      1
*DATABASE_SLEOUT
1.0000E-03      1
*DATABASE_BINARY_D3PLOT
$$ DT/CYCL      LCDDT      BEAM      NPLTC
1.0000E-03
      0
*NODE
      1      -17.8038      44.11536      -5.6208
      2      54.53807      9.184963      5.321385
      3      54.538      9.185      5.154101
      4      54.538      9.185      4.986802
      5      54.538      9.185      4.819503

.....
.....
.....
230438 24.321790005316 0.5383733641691 -0.423785316713
230439 24.313365290926 0.5402206805621 -0.251055749391
230441 24.45014481584 0.4926461266713 -0.27305628118
230442 24.442902045946 0.4970673060488 -0.438509342539

```

```

*MAT_PLASTIC_KINEMATIC
$HMNAME MATS      1steel 1020
                17.3300E-0435933000.0      0.3  86240.0

*PART
$HMNAME COMPS      1Chassis
$HWCOLOR COMPS      1      7

                1      1      1
$HMNAME COMPS      2Gussets
$HWCOLOR COMPS      2      49

                2      2      1
                5      4      1

*SECTION_SHELL
$HMNAME PROPS      1chassis section
                1      0      0.0
                0.12      0.12      0.12      0.12

*SECTION_SHELL
$HMNAME PROPS      2Gusset section
                2      0      0.0
                0.15      0.15      0.15      0.15

*RIGIDWALL_PLANAR_ID
$HMNAME GROUPS      3Front wall
$HWCOLOR GROUPS      3      22
                3
                0
                67.418      6.185-2.8350132      66.418      6.185-2.8350131

*RIGIDWALL_PLANAR_ID
$HMNAME GROUPS      4bottom wall
$HWCOLOR GROUPS      4      53
                4
                0
-0.0032435-0.43971178.55183096-0.00324350.560288268.55183096

*ELEMENT_MASS
$HMNAME COMPS      7ele_mass_driver
$HWCOLOR COMPS      7      17
    118331      32733      0.02159      7
    118332      32738      0.02159      7
    118333      32742      0.02159      7

.....
.....
    118500      16937      0.0129534      7
    118501      17095      0.0129534      7
    118502      17125      0.0129534      7
    118503      17128      0.0129534      7

*ELEMENT_SHELL
    1      1      66554      66555      66553      66553
    2      1      62539      62536      62538      62538
    3      1      61448      58454      49570      49570
    4      1      61150      61350      61149      61149

```

```

.....
116501      5  229081  229078  11208  11208
116502      5  11191  228941  228938  228938
116503      5  64048  229432  64049  64049
*ELEMENT_SHELL
  1054      1  66565  66564  66566  66567
  1055      1  66549  66565  66567  66550
  1056      1  66567  66566  66526  66525
  1057      1  66550  66567  66525  66524
.....

```

```

.....
118328      1  230442  32906  32823  32824
118329      1  32903  230441  230439  32969
118330      1  230441  32903  32826  32825
*ELEMENT_SOLID
  115866     3  227774  227763  227782  227784  227854  227843
227862  227864
  115867     3  227784  227782  227783  227785  227864  227862
227863  227865
  115868     3  227763  227762  227778  227782  227843  227842
227858  227862
.....

```

```

.....
116485      4  228398  228399  228427  228419  228432  228428  228431
228433
  116486      4  228399  228400  228426  228427  228428  228429
228430  228431

```

```

*INITIAL_VELOCITY_NODE
$HMNAME LOADCOLS      1autol
$HWCOLOR LOADCOLS      1      3
      1      265.0      0.0      0.0
      2      265.0      0.0      0.0
      3      265.0      0.0      0.0
      4      265.0      0.0      0.0
.....

```

```

.....
      230438      265.0      0.0      0.0
      230439      265.0      0.0      0.0
      230441      265.0      0.0      0.0
      230442      265.0      0.0      0.0
.....

```

```

*END

```

VITA

Graduate College  
University of Nevada, Las Vegas

Nagurbabu Noorbhasha

Degree:

Bachelor of Technology, Mechanical Engineering, 2003  
J N T University, Hyderabad, India

Thesis Title: Computational Analysis for Improved Design of an SAE Baja  
Frame Structure

Thesis Examination Committee:

Chairperson, Dr. Brendan J O'Toole, Ph. D  
Committee Member, Dr. Mohammed Trabia, Ph. D  
Committee Member, Dr. Reynolds Douglas, Ph. D  
Graduate Faculty Representative, Dr. Aly M Said, Ph. D